Journal of South American Earth Sciences 124 (2023) 104255

Contents lists available at ScienceDirect

Journal of South American Earth Sciences

journal homepage: www.elsevier.com/locate/jsames

The poly-orogenic Paleozoic rocks of Cuesta del Rahue area (Precordillera Neuquina, Argentina) and their significance in marking the southern end of the Chanic orogenic belt

Nemesio Heredia [a,*], David Pedreira [b], Raúl Giacosa [c], Samanta Serra-Varela [d], Nicolás Foix [e], José Allard [e], Pablo González [f], Fidel Martín-González [g]

[a] Instituto Geológico y Minero de España (IGME-CSIC), C/ Matemático Pedrayes 25, 33005, Oviedo, Asturias, Spain
[b] Departamento de Geología, Universidad de Oviedo, C/ Jesús Arias de Velasco s/n, 33005, Oviedo, Spain
[c] Servicio Geológico y Minero Argentino (SEGEMAR) y Universidad Nacional de Río Negro, Instituto de Investigación en Paleobiología y Geología, General Roca, Rio Negro, Argentina
[d] Universidad Nacional de Río Negro, Instituto de Investigación en Paleobiología y Geología, Av/ Roca 1242, 8332, General Roca, Río Negro, Argentina
[e] Universidad Nacional de la Patagonia, Km 4, 9000, Comodoro Rivadavia, Chubut, Argentina
[f] CONICET - Servicio Geológico y Minero Argentino (SEGEMAR), Parque Industrial General Roca, Rio Negro, Argentina
[g] Área de Geología, Universidad Rey Juan Carlos, C/ Tulipán s/n, 28933, Móstoles, Madrid, Spain

ARTICLE INFO

Keywords:
Paleozoic
Andean basement
Precordillera Neuquina
Stratigraphy
Structure
Magmatism
Chanic orogen
Gondwanan orogen

ABSTRACT

In the Cuesta del Rahue area, located in the Precordillera Neuquina (northern Argentine Patagonia), late Paleozoic turbiditic rocks with maximum depositional age of ca. 389 Ma were affected by three orogenic events. The oldest orogenic event is the Chanic orogeny (Late Devonian–early Carboniferous) that is characterized by folds with NNE vergence. This deformation is developed in low-grade to very low-grade metamorphic conditions, which allowed the development of a slaty/rough cleavage. The main Chanic structure is an asymmetric fold with a large normal limb tilted by the more recent orogenic events. The characteristics of the deformation and metamorphism allows us to assign the Cuesta del Rahue outcrop to the external hinterland of the western wedge of the Chanic orogen. Early to late Carboniferous igneous rocks intruded the Paleozoic rocks of the Cuesta del Rahue area and crosscut the Chanic structures. After the Chanic orogeny, the Gondwanan orogeny (late Carboniferous–early Permian) took place. The main structures of the Gondwanan orogen are thrust and related folds with SSW vergence that fold the large Chanic normal limb and also affect Carboniferous igneous rocks. The Gondwanan deformation was developed under non-metamorphic conditions, and Permian igneous rocks crosscut the Gondwanan structures. Mesozoic regional extension related to the beginning of the Andean cycle and the formation of the Neuquén Basin gave rise to normal faults and small-scale extensional folds. Finally, the Andean orogeny, developed during the Cenozoic in the study area, also affected the Cuesta del Rahue Paleozoic rocks, with the development of compressional structures related to the Aluminé thrust and fold belt. The main Andean structure in the study area is the NW–SE Rahue fault, which links the E–W Piedra Santa tear fault with the NNE–SSW Cantan Lil reverse fault. The Rahue fault has a SW tectonic transport direction. It uplifted the Cuesta del Rahue area and placed Paleozoic rocks on top of Mesozoic and Cenozoic rocks. The Piedra Santa fault partially reactivated the Huincul right-lateral and left-lateral Chanic transverse faults that define the southern end of the doubly vergent Chanic orogen, giving rise to the current Huincul lineament.

1. Introduction

The Andes are a complex mountain range formed after several subduction and collision orogenic events with different spatial and temporal imprints along the western border of the South American Plate. Although a great effort has been made in the last 15 years to shed some light on the understanding of the distribution and effects of each orogenic cycle, especially those of the Paleozoic (e.g. Heredia et al.,

* Corresponding author.
E-mail address: n.heredia@igme.es (N. Heredia).

https://doi.org/10.1016/j.jsames.2023.104255
Received 15 November 2022; Received in revised form 7 February 2023; Accepted 8 February 2023
Available online 15 February 2023

2016, 2018a,b), there are still large areas where this knowledge remains elusive, hampering a comprehensive view of the poly-orogenic evolution of this mountain belt.

Between the Southern and Central Andes (Fig. 1A and B), the Huincul lineament is a prominent but still quite enigmatic ~E–W morphostructual feature that marks the southern border of the Huincul Intraplate Deformation Zone, located in the southern margin of the Mesozoic–Cenozoic Neuquén basin (Mosquera et al., 2011; Guzmán et al., 2021; Rossello and López de Lucchi, 2022 and citations therein). The Huincul lineament also separates different sectors of the Andean Paleozoic basement: the Cuyo Sector to the north and the Patagonian Sector to the south (Heredia et al., 2016). The Cuyo Sector was affected during the late Paleozoic by the Chanic collisional orogeny (Late Devonian-early Carboniferous) and the subduction-related Gondwanan orogeny (late Carboniferous–middle Permian), while the Patagonian Sector is only affected by the Gondwanan subduction-collision orogeny,

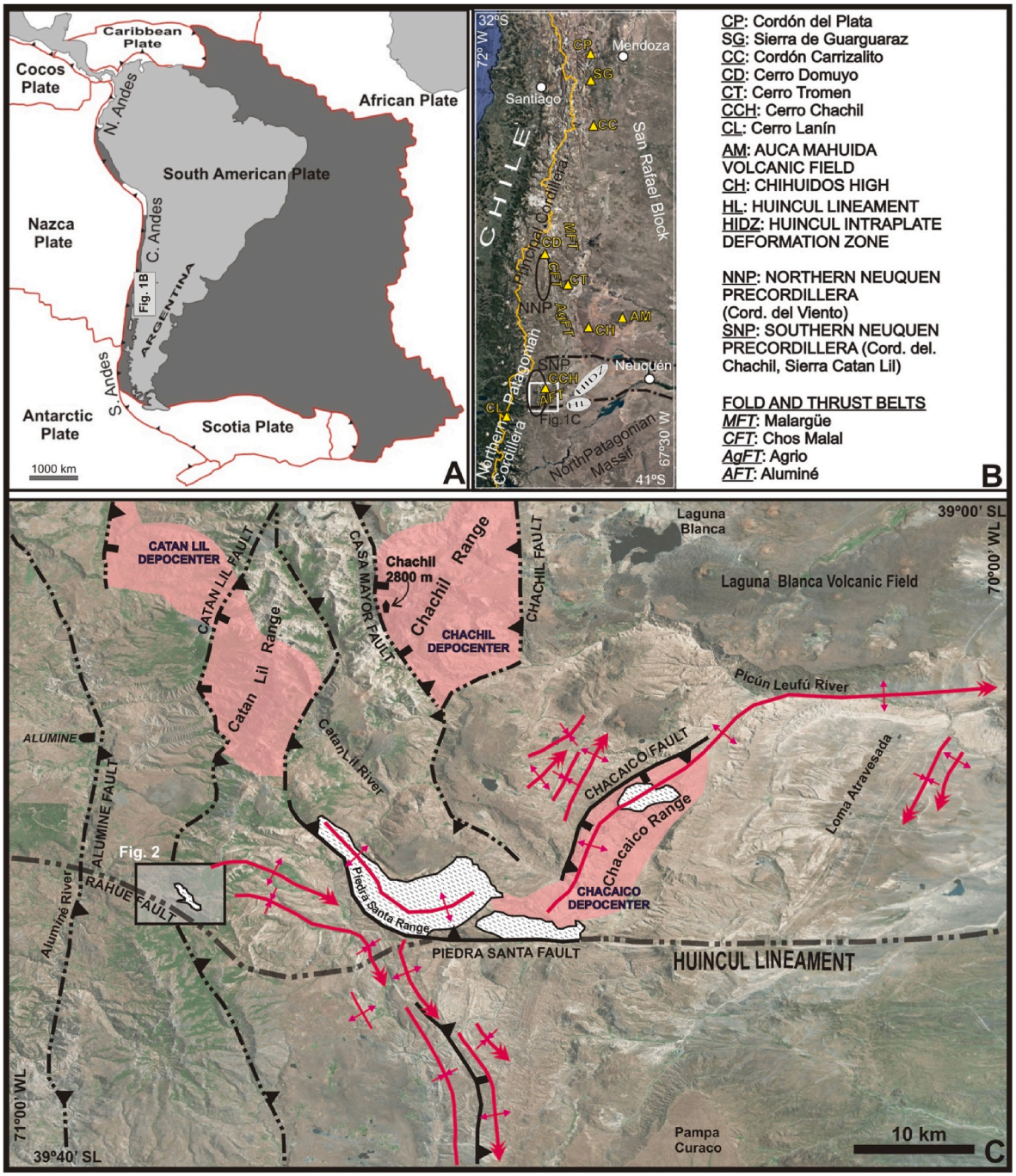

Fig. 1. (A) Study area location in South America. (B) Bing Image with the location of geological regions, structural sectors, and the main ranges and hills in the western part of the Neuquén and Mendoza provinces. The study area is at the intersection between the Southern Neuquén Precordillera and the Huincul intraplate deformation zone (Huincul Ridge), N–S and W–E-oriented, respectively. The white square indicates the location of Fig. 1C. (C) Main structures in the region surrounding the study area. The Chachil and Catán Lil ranges are depicted, which are part of the Southern Neuquén Precordillera with N–S oriented structures and other structures with different orientations associated with the Huincul intraplate activity. Outcrop areas with Paleozoic metamorphic rocks (with white background) and "precuyanos" depocenters from the Late Triassic–Early Jurassic (pale pink) are approximately located. The black square indicates the location of the study area and the geological map of Fig. 2.

which started earlier (Middle Devonian–early Permian) (Heredia et al., 2016, 2018b). Finally, during the Andean cycle, Permian–Cenozoic in age in the study area and throughout the Cuyo Sector, the Andes acquired their current architecture and the Paleozoic structures were reactivated in some segments, both during the pre-orogenic (mainly Mesozoic) and orogenic (mainly Cenozoic) stages of this cycle (e.g. Rodríguez-Fernández et al., 1997; Giambiagi et al., 2014;Giacosa et al., 2014).

In spite of the tectonic relevance of the Huincul lineament during the Paleozoic orogenic events, its continuation toward the west of the Paleozoic outcrops of the Piedra Santa Range (Fig. 1C) is not well known. In this area, another small outcrop of Paleozoic rocks in Cuesta del Rahue stands out as a key place to shed light onto the geodynamic evolution of the Paleozoic orogenies, and is the subject of this study.

We carried out a multidisciplinary approach to characterize the polyorogenic Paleozoic basement rocks of the Cuesta del Rahue area and surroundings through new geological mapping and detailed structural, sedimentological, petrological and geochronological analyses. The detailed structural work (Cuesta del Rahue structural section) was carried out along the RP-46 road, at the end of the rise of Rahue (last seven curves of the ascent to the Rahue pass), located between 1276 and 1470 m a.s.l.

The main aim of our work is to specify the age of these rocks and correlate them with those that crop out in nearby areas, in order to establish: (i) the type, conditions, and age of the deformation; (ii) the relationships between deformation and metamorphism; and (iii) the orogenic cycles to which the outcropping units belong and their position within the respective orogenic belts. The final goal is to propose an updated and better constrained geodynamic evolution model for the southwestern margin of Gondwana at these latitudes.

2. Geological setting

2.1. Location of study area

The study area is located in the northwestern region of the Argentine Patagonia, between 39°20' and 39°25' S latitude, in the western part of the Neuquén province, about 50 km from the Chilean border (Fig. 1A).

Cuesta del Rahue is located in the southwestern slope of the Catán Lil range (Fig. 1C). This range along with the Piedra Santa and Chachil ranges integrate the geographical and geological region of the Southern Neuquén Precordillera (SNP). This región together with the Northern Neuquén Precordillera (NNP), where Cordillera del Viento stands out, form an area that is separated from the Principal Cordillera de los Andes and is known as Precordillera Neuquina (Ramos et al., 2011). The Precordillera Neuquina presents average elevations above 2000 m a.s.l. and around 3000 m a.s.l. in the Cordillera del Viento (NNP), which culminates in the 4709 m a.s.l. of the Cerro Domuyo peak, the highest one in the Argentine Patagonia (Fig. 1B). The SNP, where Cuesta del Rahue area is located, includes also the western part of the Huincul intraplate deformation zone or Huincul Ridge (Fig. 1B and C). At the Cuesta del Rahue latitude, the SNP is separated from the Northern Patagonian Cordillera by the longitudinal valley of the Aluminé river (Fig. 1C).

2.2. Regional stratigraphy

The regional stratigraphic framework can be divided into three major lithological associations: a Paleozoic metasedimentary and igneous basement, a Mesozoic sedimentary and volcanic sequence, and a Cenozoic volcanic and sedimentary sequence.

The Paleozoic basement is composed of pre-Carboniferous metamorphic rocks and Carboniferous–Permian plutonic rocks. Different authors assigned different names, ages and/or lithostratigraphic features to the metamorphic rocks, making the tectonic interpretations difficult. The outcrops in the Piedra Santa and Chacaico ranges (Fig. 1C) were assigned to the Silurian–Devonian Piedra Santa Formation (Digregorio and Uliana, 1980) by Leanza et al. (1997) and Cucchi et al. (2005), whereas the ones cropping out in the Cuesta del Rahue area were assigned to the Colohuincul Formation by Turner (1976) with an imprecise age ranging from the Precambrian to the Paleozoic (see Cingolani et al., 2011 and citations therein). Franzese (1995) gathered under "Piedra Santa Complex" several outcrops of metamorphic rocks from the precordilleran and cordilleran zones, although distant from each other. Franzese (1995) also separated three parts within this complex: the Piedra Santa Formation, the Rahue-Ñorquinco-Rucachoroi Series, and the Quillén Series; being the first two located in the study area and their surroundings, and the last one further west. This author also proposed an age between the Silurian and the Middle Devonian for the Piedra Santa Formation, considering the ages of its metamorphism, developed between the Late Devonian and early Carboniferous (Table 1).

In the Piedra Santa range, the Paleozoic metamorphic rocks developed under low pressure and intermediate temperature conditions, reaching a medium metamorphic grade. They include metapelitic rocks and meta-sandstones, with some volcanic intercalations ranging from meta-andesites to meta-basalts (Franzese, 1995). In addition, large areas affected by a contact metamorphism can be observed in this zone, with the presence of hornfels and spotted and porphyroblastic schists with cordierite and andalusite (Franzese, 1995). In the Rahue area, rocks display a very low metamorphic grade and are mainly metasandstones with thin intercalations of slates (Franzese, 1995) with a depositional age not older than Late Devonian (Ramos et al., 2010).

The Paleozoic plutonic rocks are predominantly granodiorites, but also granites, tonalites, tonalite porphyries, and quartzdiorites in minor proportion, which were grouped in the Chachil Plutonic Complex (Leanza, 1992). These rocks intrude the Piedra Santa and Rahue metamorphic rocks and occupy most of the adjacent Chachil and Catán Lil ranges (Fig. 1C), with ages between the late Carboniferous, ca. 303 Ma (late Pennsylvanian) and the early Permian, ca. 285 Ma (Varela et al., 1994; Romero et al., 2020) (Table 1).

Mesozoic rocks unconformably overlie the Paleozoic basement and were deposited in an extensional context. They constitute the pre-orogenic succession of the Andean orogenic cycle, beginning with two syn-rift volcano-sedimentary sequences dominated respectively by pyroclastic rocks and continental clastic rocks and assigned to the Choiyoy and Lapa formations (Leanza et al., 1997; Cucchi et al., 2005) (Fig. 2). The oldest one belongs to the late Permian–Early Triassic and the youngest one to the Late Triassic–Early Jurassic, being part of the "Precuyano" sedimentary cycle, as Leanza et al. (2005) and Franzese et al. (2011) proposed. A great portion of these rocks crop out extensively throughout the eastern and western margins of both the Chachil and Catán Lil ranges, as well as in the Chacaico and Piedra Santa ranges (Fig. 1C).

The Cuyo Group unconformably overlies the Precuyano cycle rocks. Their deposits are well exposed throughout the study area (Los Molles Formation in Fig. 2) and represent the initial infill of the Neuquén Basin in Early Jurassic times. The Neuquén Basin is characterized by a thick sedimentary succession that reach the Early Cretaceous, in which marine and continental deposits alternate. The Cuyo Group composes the first complete marine transgressive–regressive cycle, which crops out extensively in a 50 km-wide belt between the Aluminé river and the eastern part of the Chacaico range. Lithostratigraphic units of this group include continental deposits and distal coastal and evaporitic marine deposits, whose sedimentation took place in the last part of the Early Jurassic and up to the Middle Jurassic. Toward the east of the Chacaico range and the south of the Piedra Santa range, there are also outcrops of different units of the Mendoza Group, forming a new sedimentary cycle with several units of continental and marine nature, whose age encompasses the Kimmeridgian–early Barremian interval (Late Jurassic–Early Cretaceous) (Cucchi et al., 2005; Naipauer et al., 2012, 2018; Pujols et al., 2018 and citations therein).

Cenozoic deposits correspond to the syn-orogenic succession of the

Table 1
Summary of radiometric ages of the Paleozoic metamorphic and igneous rocks in the Chachil and Piedra Santa ranges and in the Cuesta del Rahue area (study area). Southern Neuquén Precordillera.

Rahue biotite-hornblende granodiorite	Rb/Sr	237 ± 70 Ma	Cingolani et al. (1991)	Middle-Upper Triassic
Chachil biotitic tonalitic porphyry	K/Ar WR	281 ± 4 Ma	Sillitoe (1977)	Lower Permian
Alumine river granitoid	Rb/Sr	285 ± 5 Ma	Varela et al. (1994)	
Chachil biotite tonalite	U–Pb U–Pb LA-MC-ICPMS (Zr)	303 ± 2 Ma	Romero et al. (2020)	Upper Carboniferous
Chachil porphyritic tonalite	Re–Os (molybdenite)	ca. 316–312 Ma	Garrido et al. (2008)	
Piedra Santa porphyritic granite	U–Pb SHRIMP (Zr)	ca. 357 Ma	Rapela et al. (2022)	Lower Carboniferous
Piedra Santa schist (thermal contact metamorphism)	K/Ar WR	299 ± 14 Ma	Franzese (1995)	Carboniferous/Permian
Piedra Santa schist (regional metamorphism)	K/Ar WR	311 ± 16 Ma		Upper Carboniferous
		329 ± 16 Ma		Lower Carboniferous
		372 ± 18 Ma		Upper Devonian
Rahue metasandstone	U–Pb SHRIMP (detrital Zr)	*ca.* 364 Ma (m.s.a.)	Ramos et al. (2010)	Upper Devonian
Rahue metasandstone	U–Pb LA-Q-ICPMS (detrital Zr)	392.1 ± 3.9 (m.s.a.)	This study	Middle Devonian
Rahue leucogranitic dikes	U–Pb SHRIMP (Zr)	306 ± 2 Ma	Hervé et al. (2018)	Upper Carboniferous
Piedra Santa metasandstone	U–Pb LA-MC-ICPMS (detrital Zr)	ca. 446 Ma (m.s.a.)	Romero et al. (2020)	Lower Silurian

WR: whole rock; m.s.a.: maximum sedimentation age; Zr: zircon

Andean orogenic cycle. In the study area, this succession gives rise to a set of andesitic lavas and tuffs, with volcanic breccia and agglomerates that crop out in the SW part of the Catán Lil range. These rocks were assigned by Turner (1976) and Cucchi et al. (2005) to the Auca Pan Formation (Eocene–early Oligocene) and by García Morabito and Ramos (2012) to the Naunauco Group (Late Cretaceous–Paleogene). Later, the deposition of continental sedimentary rocks took place with abundant interbedded volcanic rocks that are part of the infill of the Bío-bío-Aluminé basin. This basin has an elongated shape with a NNW trend that reaches 38°S in Chile, cropping out in the Argentine Andes west of the Catán Lil range and in the Aluminé river depression. In this basin, from bottom to top, three formations can be separated: the basaltic lavas and sediments of the late Oligocene Rancahue Formation; the alluvial and pyroclastic deposits of the Chimehuín Formation, Miocene in age; and the basaltic lavas of the late Miocene Tipilihuque Formation (Franzese et al., 2011). Specifically, the clastic sediments of the Chimehuín Formation are clustered in some isolated depocenters near the study area, such as the Catán Lil depocenter (García Morabito and Ramos, 2012) (Fig. 1C).

2.3. Regional structure

According to Franzese (1995), the structure of the Paleozoic metamorphic rocks of the Piedra Santa range is the result of a ductile polyphasic deformation, in which four phases can be identified. Three of these deformation phases (D1 to D3) were previous to the intrusion of late Carboniferous granitoids and developed under low pressure/intermediate temperature metamorphic conditions, which reached the medium grade. The D4 was developed after the intrusion of the granitoids, in the brittle-ductile transition and under conditions of very low metamorphic grade. During the D1 phase, a first cleavage (S_1) related to isoclinal folds was formed, which was followed by a second pervasive cleavage (S_2), related to isoclinal and sheath folds developed in shear zones. The D3 phase gave rise to a crenulation cleavage (S_3) associated with closed to open folds. Subsequently, the D4 phase led to a spaced cleavage (S_4) related to kink-type folds. Finally, a brittle deformation (D5), developed in absence of metamorphism, gave rise to large-scale folds and regional faulting, and might be related to the Andean orogenic cycle.

According to Heredia et al. (2016, 2018a) the Paleozoic rocks of the Cuesta del Rahue area must constitute a poly-orogenic basement deformed by either the Famatinian collisional orogeny (Late Ordovician–middle Silurian) or by the Chanic subduction-collision orogeny (Middle Devonian–early Carboniferous), depending on whether we consider it located (something to be determined): in the Cuyo or in the Patagonian sectors, respectively. The study area was later affected by the Gondwanan orogeny, which shows different characteristics and timing in the Cuyo Sector (a late Carboniferous–early Permian subduction orogeny) and in the Patagonian Sector (Late Devonian–early Permian subduction-collision orogeny).

In Late Triassic times, the Andean orogenic cycle began around the study area with an initial rifting phase that started to develop the Neuquén Basin. This rifting phase gave rise to several isolated NW–SE half grabens (Vergani et al., 1995) with three main depocenters: Catán Lil, Chacaico, and Chachil (Fig. 1C). The Chacaico depocenter, located in the Huincul Ridge, is one of the few with a NNE orientation and is controlled in its western edge by the Chacaico fault and by a group of W–E to WNW–ESE minor faults, which delimit its half graben geometry (Franzese et al., 2007). The Chachil and Catán Lil depocenters present the classic pattern of most depocenters in the Neuquén Basin, which are limited by first order NNW normal faults, and second order ENE- and NE-oriented faults (Hernández et al., 2022).

Many of the structures of the Mesozoic rift phase, particularly the main faults that delimit the half grabens, were reactivated during the compressive stage of the Andean cycle or Andean orogeny (e.g. Catan Lil, Chachil, Casa Mayor and Chacaico faults, among others, Fig. 1C).

The Andean orogeny developed the Aluminé Fold and Thrust Belt (ALFTB) in Late Cretaceous and late Miocene to Pliocene times (García Morabito and Ramos, 2012), with an intercalated intraorogenic extensional stage, Oligocene to early Miocene in age, in which thick volcano-sedimentary sequences accumulated (Franzese et al., 2007). This extensional stage has also been recognized further south by Giacosa and Heredia (2004) and Giacosa et al. (2005).

The internal domain of the ALFTB, located westward of the long depression of the Aluminé river valley, west of the study area, is a basement-involved Andean belt, characterized by N to NNE thrusts with tectonic transport to the E and no evidence of tectonic inversion (García Morabito and Ramos, 2012).

The external domain of the ALFTB is located in the Southern Neuquén Precordillera, where the study area is located. This domain is characterized by reverse faults with tectonic transport toward the west (backthrusts), many being the product of the tectonic inversion of Mesozoic normal faults. This inversion allowed for the current outcrops of the pre-rift Paleozoic basement sequences and the syn-rift and post-rift Mesozoic sequences (García Morabito and Ramos, 2012). Although the structures of this domain are mainly N–S to NNW–SSE trending, in a wide area located eastward of the Cuesta del Rahue area, the sedimentary cover shows structures with different orientations, due to the influence of the southern edge of the Huincul Ridge: the Huincul lineament (Fig. 1).

The propagation of the deformation toward the foreland and the interaction with the Huincul Ridge produced curved structural geometries in the ALFTB, like the Piedra Santa and Chacaico faults and others like the W–E-oriented Picún Leufú anticline (Fig. 1C). The Huincul Ridge is interpreted in the context of a dextral transcurrent zone, a lateral structure that conditioned the development of the Andean thrust and

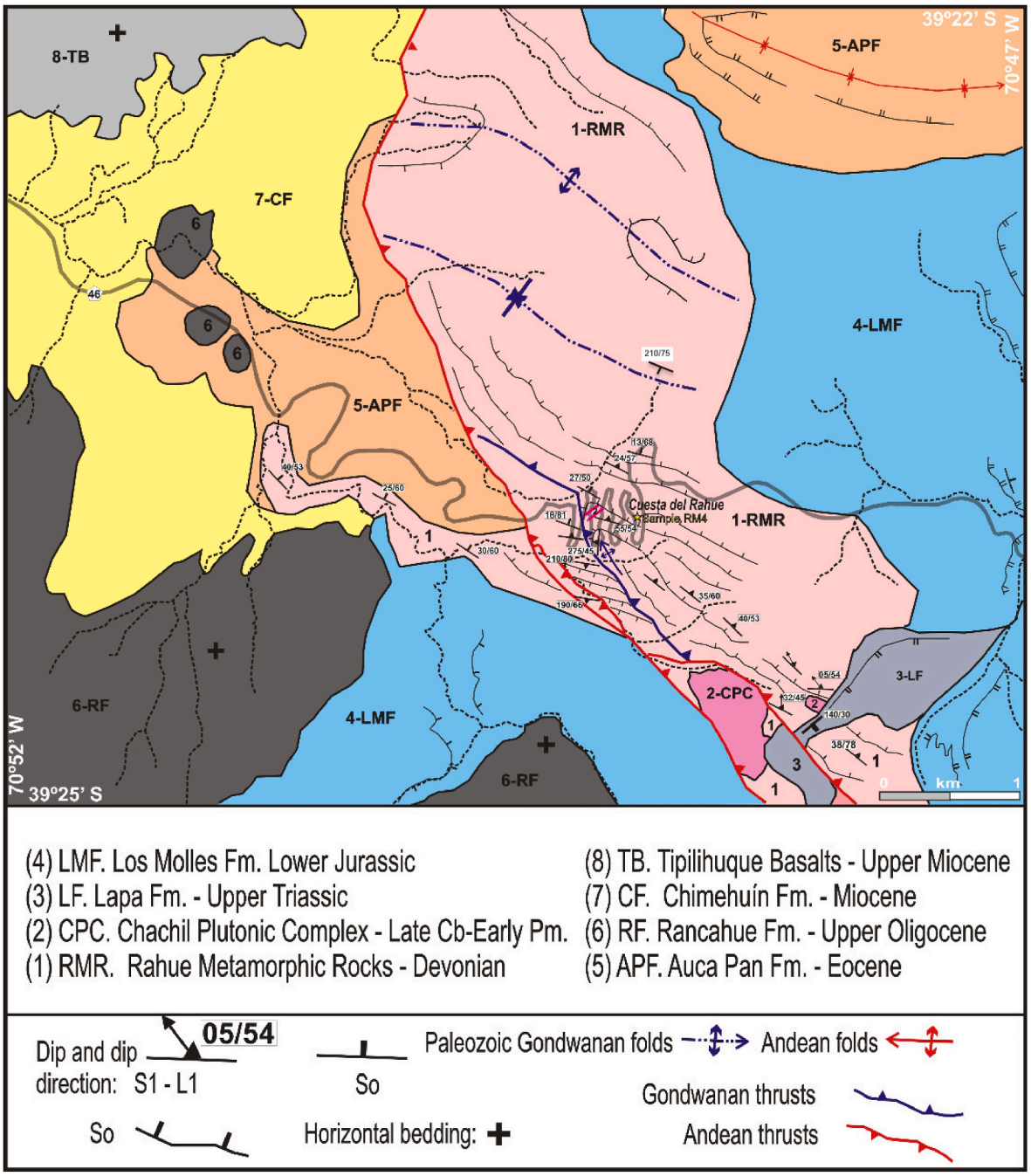

Fig. 2. Geological map and main structures of the study area (Cuesta del Rahue and surroundings). Boundaries between the Cenozoic rocks are modified from Turner (1976) and Cucchi et al. (2005). Nomenclature and age of Cenozoic rocks according to Franzese et al. (2011). Location in Fig. 1C.

fold belt in this area (Rossello and López de Luchi, 2022).

3. The Paleozoic rocks of the Cuesta del Rahue area

In the Cuesta del Rahue area, a NNW–SSE basement block crops out, limited by Andean back thrusts at its southwestern edge and unconformably covered by Mesozoic and Cenozoic rocks at the rest (Fig. 2). This basement block is mainly composed of Paleozoic metamorphic rocks and, in its southern part, by Carboniferous–Permian granitoids (Fig. 2).

3.1. The metasedimentary rocks

The Paleozoic metasedimentary rocks of Cuesta del Rahue are composed of a monotonous alternance of phyllites and metasandstones with subordinate metaconglomerates. The very low-grade metamorphic conditions of these rocks allow us to carry out stratigraphic-sedimentological studies to approximate their depositional environment. This sequence also crops out in the northwestern part of the Piedra Santa area (Fig. 1C).

3.1.1. Metasedimentary sequence

The metaconglomerates are generally poorly sorted, massive, not imbricated, matrix supported, with fine-medium sub-rounded to angular intrabasinal gravel clasts (Fig. 3A). They mainly occur as basal deposits of fining-upward metasandstone bodies. Most of the metasandstones are tabular, massive (Fig. 3B), no-graded bodies with planar base, ranging about 0.1–0.5 m in thickness. Metasandstones also can be lobulated

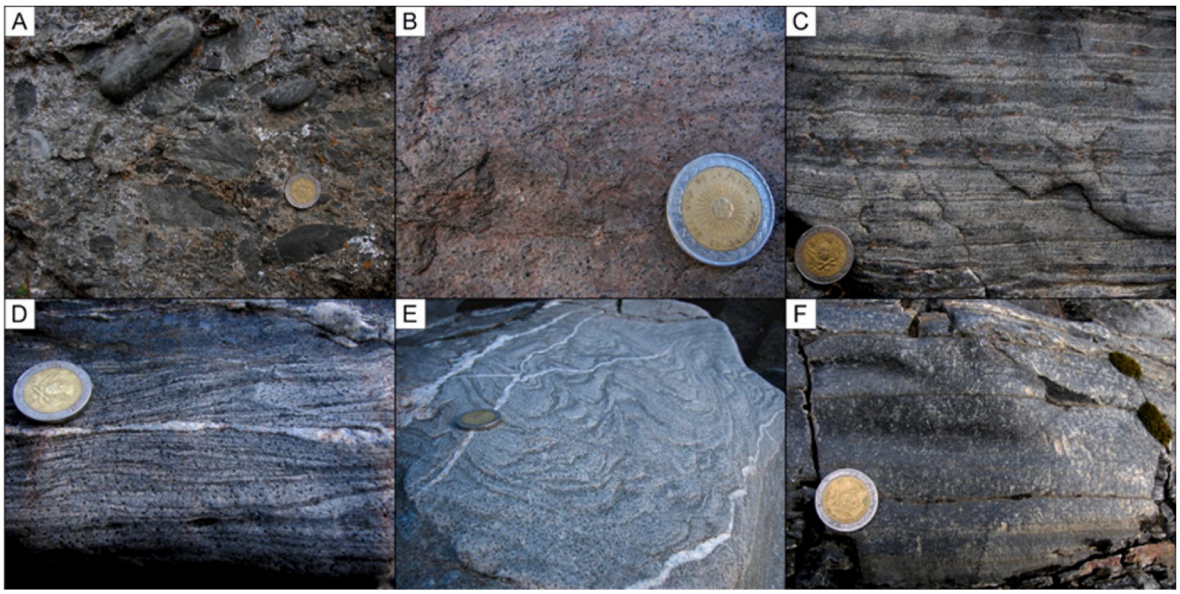

Fig. 3. Photographs of the main lithologies of the metasedimentary sequence of the Cuesta del Rahue area and their surroundings. Coin is 2 cm in diameter. (A) Massive, matrix-supported metaconglomerates. (B) Massive metasandstones. (C) Planar laminated metasandstones. (D) Ripple cross-laminated sandstones. (E) Small-scale soft-sediment deformation structures by water scape. (F) Massive and laminated metapelites.

bodies displaying topographic compensation. Some bodies that reach up to 2.5–3 m in thickness can contain erosional bases and fining-upward tendency. Metasandstones can also have planar lamination (Fig. 3C) or ripple cross-lamination near the top (Fig. 3D), with eventual small-scale soft-sediment deformation structures (Fig. 3E). The strata of metapelites are massive or laminated (Fig. 3F). The metasedimentary succession of the Cuesta del Rahue area displays 10–20 m thick, coarsening and thickening-upward stratigraphic cycles (Fig. 4) and shows a normal polarity.

A rhythmic alternation of traction/decantation are the dominant sedimentary processes in the metasedimentary succession of the Cuesta del Rahue area. The gradation from massive to planar- and micro-laminated sandstones represents a non-confined flow transformation from high/hyper-concentrated to diluted/turbulent upper-to-lower regime conditions. Erosive, fining-upward bodies from metaconglomerates to metasandstones are interpreted as subaqueous channelized deposits. These bodies show simple or multistorey geometries, the latter is evidence of local avulsion and reoccupation of the feeder channel system.

Deciphering the stratigraphic and the sedimentological cycles of the nested depositional cycles observed in the study area requires high-resolution stratigraphy that is beyond the scope of this contribution. However, all described sedimentary features are consistent with deep-water turbiditic fan deposits (i.e. Walker, 1992; Mutti et al., 2009). The presence of conglomerates and the predominance of sandstones over pelites is interpreted as indicator of proximality in the sedimentary system. The coarsening and thickening-upward stratigraphic cycles are interpreted as the progradation of the turbiditic-fan complexes in a Paleozoic sedimentary basin, probably located in the eastern margin of the Chilenia subplate (in the sense of Heredia et al., 2018a).

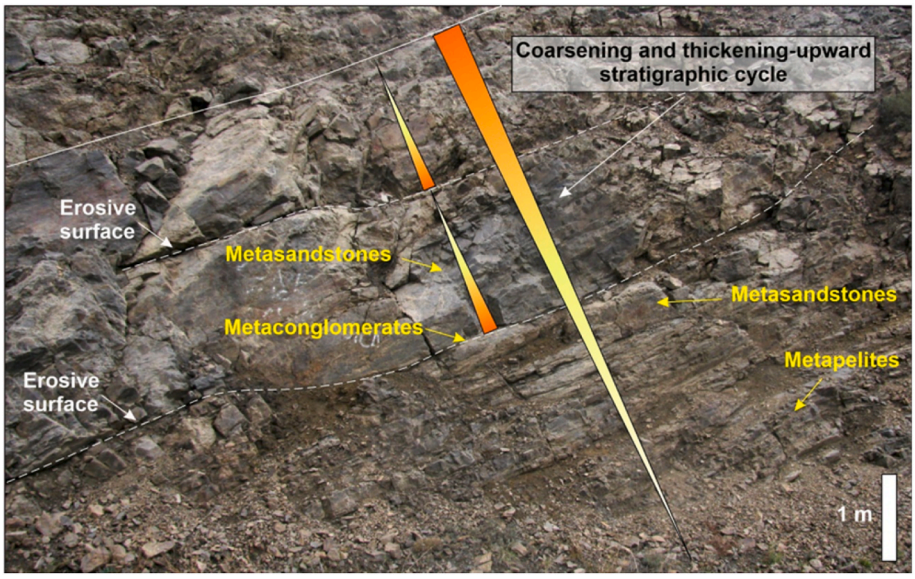

Fig. 4. The metasedimentary succession of the Cuesta del Rahue section displays decameter-scale coarsening- and thickening-upward stratigraphic cycles. The scour structure with coarse-grained lag deposits defines the stratigraphic way-up of the beds in the folded sequence.

The Paleozoic rocks of the Cuesta del Rahue area were unconformably covered by Mesozoic–Cenozoic volcanic and sedimentary rocks that constitute the Andean cover (Fig. 2). A small part of this cover is represented by the Late Triassic Lapa Formation, which crops out in the southeastern part of the study area and is composed of volcanic breccias with granitic and metamorphic lithoclasts (Fig. 5A and B). The whole eastern part of the study area and most of the southern edge of the Cuesta del Rahue tectonic block are covered by lutites and limestones of the Los Molles Formation, Early Jurassic in age (Figs. 2 and 5C). The rest of the outcrops are Cenozoic sedimentary and volcanic rocks, starting with Eocene volcanic rocks of the Auca Pan Formation (Fig. 2). This formation overlies the Los Molles Formation in angular unconformity and is in tectonic contact with the Paleozoic metamorphic rocks of the Cuesta del Rahue area. Lavas from the Rancahue Formation, late Oligocene in age (Figs. 2 and 5D) crop out in the southern part and Miocene continental sedimentary rocks and basalts of the Chimehuin and Tipilihueque formations (Figs. 2 and 5D) can be observed in the western part (Franzese et al., 2011, Fig. 2).

3.1.2. U–Pb geochronology of metasedimentary rocks

We analyzed a sample of a metasandstone collected in the Cuesta del Rahue section (coordinates: 39°23'54.5″S, 70°48'51.3″W) with a paragenesis of Qz + Pl + Ms + Bt. Porphyroblasts of biotite can be found surrounded by a rough cleavage defined by fine flakes of biotite and muscovite. Moreover, chlorite replacing biotite can be found as a secondary phase and opaque minerals and zircon are present as an accessory phases.

3.1.2.1. Analytical method. U–Th–Pb isotope and elemental measurements of zircon detrital grains were conducted by LA-Q-ICPMS at the SGIker-Geochronology and Isotope Geochemistry Facility of the University of the Basque Country (Spain). Standard jaw crushing, sieving, and heavy mineral concentration by hydraulic processes and magnetic susceptibility techniques were performed at the laboratories of the Instituto de Paleobiología y Geología (National University of Río Negro, Argentina). The concentrate was purified by hand picking. About 120 zircon grains of the sample were cast on a mount, polished, and documented using optical (reflected and transmitted light) and scanning electron microscopy (backscattered electrons). Backscattered electron images (BSE) were obtained with a JEOL JSM 5600 scanning electron microscope of the University of Oviedo, in order to assess the internal morphology, prior to the U–Pb laser work.

The samples were ablated with an Applied Spectra RESOlution M50 193 nm UV ArF excimer laser system coupled to a Thermo Fisher iCAP Qc quadrupole ICP-MS instrument with enhanced sensitivity through a dual pumping system. Spot diameters of 24 μm in zircons, repetition rates of 5 Hz, and laser fluence at the target of ca. 6 J/cm^2 were employed. The ablated material was carried in helium and nitrogen, then mixed with argon prior to injection into the plasma source. The signals of ^{202}Hg, ^{204}(Pb + Hg), ^{206}Pb, ^{207}Pb, ^{208}Pb, ^{232}Th, and ^{238}U masses were acquired. The occurrence of common Pb in the samples was monitored by the evolution of ^{204}(Pb + Hg) signal intensity. Single analyses consisted of 25 s of background integration with laser off followed by 45 s integration with the laser firing and a 30 s delay to wash out the previous sample (ca. 10 s for 6 orders of magnitude) and prepare the next analysis.

Data reduction was carried out with Iolite v. 3.6 (Paton et al., 2011) and VizualAge (Petrus and Kamber, 2012) using GJ-1 zircon standard (Jackson et al., 2004) for calibration and Plesovice zircon (Sláma et al., 2008) as secondary standard. For each analysis, the time-resolved signal of single isotopes and isotope ratios were monitored and carefully inspected to verify the presence of perturbations related to inclusions, fractures, mixing of different age domains or common Pb. The concentrations of U–Th–Pb were calibrated relative to the certified contents of GJ-1 zircon standard (Jackson et al., 2004). Percentage concordance was calculated as [(^{206}Pb/^{238}U age)/(^{207}Pb/^{206}Pb age)] × 100 (Meinhold et al., 2010). Age calculation and plots were made using ISOPLOT software (Ludwig, 2003). For further details of the analytic procedures, see Puelles et al. (2014). All analytical errors are presented as absolute values at 2σ level (Table 2).

3.1.2.2. Results. One hundred and five spots were analyzed from different zircons, out of which twenty-six were discarded for being discordant and having high common Pb contents. Most of the analyzed zircons have subhedral prismatic shapes with rounded tips and sizes ranging from 100 to 200 μm and aspect ratios of 2:1 to 3:1. In the BSE images, these zircon grains show oscillatory zoning that can be attributed to magmatic textures. Also, it is common to find inclusions in these

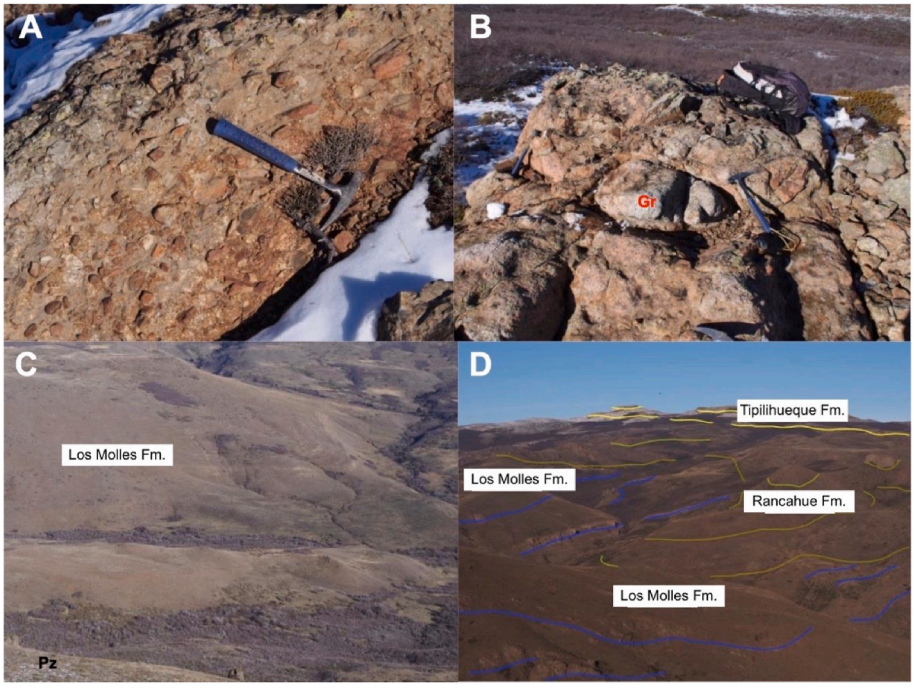

Fig. 5. Photographs of main Mesozoic and Cenozoic rocks of the Cuesta del Rahue area and their surroundings. (A) Late Triassic Lapa Formation with basement clasts of metamorphic and igneous rocks. (B) Lapa Formation with a big clast of an igneous rock (Gr). (C) Alternation of limestones (gray beds), sandstones, and lutites in the Early Jurassic Los Molles Formation in the footwall of the Rahue fault. Pz. Paleozoic outcrops of the Cuesta del Rahue (Hanging wall of the Rahue fault). (D) Unconformity between Los Molles Formation (Early Jurassic) and the Rancahue Formation (late Oligocene). The Tipilihueque basalts (Miocene) can be seen at the top of the mountains. View to the south from Cuesta del Rahue.

Table 2
U–Pb analysis results in detrital zircon grains of sample RM4, obtained in a metasandstone of the Cuesta del Rahue section. Location coordinates: 39°23′54.5″S - 70°48′51.3″W (Fig. 2).

Spot	207 Pb/ 235U	2SE (abs)	206 Pb/ 238U	2SE (abs)	Rho	238U/ 206 Pb	2SE (abs)	207Pb/ 206 Pb	2SE (abs)	% conc	[U] (μg g-1)	[Th] (μg g-1)	[Pb] (μg g-1)
L_20_03_06–1	2.264	0.07	0.2073	0.004	0.4606	4.823927	0.09308107	0.0802	0.0022	101%	61.3	14.29	63.7
L_20_03_06–2	0.527	0.014	0.0667	0.0011	0.45642	14.9925	0.2472527	0.0574	0.0015	97%	393	111.6	160.9
L_20_03_06–3	1.615	0.034	0.1645	0.0028	0.74865	6.079027	0.1034728	0.07181	0.0012	101%	434	86	304
L_20_03_06–5	0.569	0.014	0.0699	0.0013	0.81726	14.30615	0.2660658	0.05915	0.001	96%	926	135.3	237
L_20_03_06–6	2.06	0.1	0.19	0.0049	0.46991	5.263158	0.1357341	0.0785	0.0033	100%	51.7	17.93	69.2
L_20_03_06–8	0.512	0.011	0.0667	0.0011	0.76947	14.9925	0.2472527	0.05559	0.00091	99%	925	306	416
L_20_03_06–11	2.147	0.044	0.2072	0.0041	0.76301	4.826255	0.09550022	0.0755	0.0013	104%	490	38.5	154.1
L_20_03_06–13	0.567	0.019	0.0668	0.0016	0.3777	14.97006	0.3585643	0.0623	0.0021	92%	885	205.7	333
L_20_03_06–14	2.744	0.064	0.2237	0.004	0.66139	4.470273	0.07993335	0.0897	0.0018	97%	175.2	102.8	478.7
L_20_03_06–16	0.843	0.019	0.1005	0.0019	0.76696	9.950249	0.1881142	0.06122	0.0011	100%	510	464	960
L_20_03_06–17	0.4798	0.0098	0.0624	0.001	0.7243	16.02564	0.2568212	0.05614	0.00096	98%	1095	152.5	220.3
L_20_03_06–18	0.559	0.018	0.0637	0.0014	0.35231	15.69859	0.3450239	0.0644	0.0021	89%	848	179	302
L_20_03_06–19	0.588	0.03	0.0712	0.0027	0.90596	14.04494	0.5326032	0.06	0.0016	95%	948	200	292.5
L_20_03_06–20	1.625	0.034	0.1635	0.003	0.75062	6.116208	0.112224	0.073	0.0013	100%	411	83.6	302
L_20_03_06–21	1.834	0.043	0.1747	0.0034	0.72149	5.724098	0.111402	0.0769	0.0015	98%	232	56.8	206.4
L_20_03_06–23	0.591	0.014	0.0678	0.0021	0.8092	14.74926	0.4568356	0.0645	0.0013	90%	1160	120.9	255
L_20_03_06–24	2.234	0.057	0.1944	0.0036	0.57721	5.144033	0.09525987	0.0843	0.0019	96%	198	153	636
L_20_03_06–30	1.913	0.045	0.1778	0.0033	0.70921	5.624297	0.104388	0.0762	0.0013	98%	369.2	74.9	307.9
L_20_03_06–31	2.101	0.043	0.1961	0.0034	0.77785	5.099439	0.08841455	0.07587	0.0012	101%	291.3	61.3	302
L_20_03_06–32	2.121	0.099	0.2029	0.0094	0.6776	4.928536	0.2283304	0.0745	0.0029	103%	299	25.77	83.4
L_20_03_06–34	0.51	0.01	0.0668	0.0012	0.65522	14.97006	0.2689232	0.05497	0.0011	100%	655	176.5	249
L_20_03_06–36	2.281	0.053	0.2017	0.0035	0.56353	4.957858	0.08603125	0.0818	0.0018	99%	135.2	47.7	208
L_20_03_06–37	1.067	0.028	0.1202	0.0024	0.78896	8.319468	0.1661125	0.0643	0.0012	99%	511.8	58	157.4
L_20_03_06–38	2.053	0.042	0.194	0.0034	0.63652	5.154639	0.09033904	0.0774	0.0015	101%	120.6	49.94	208.1
L_20_03_06–40	0.496	0.01	0.0656	0.0012	0.70817	15.2439	0.2788519	0.05558	0.00099	100%	821	256	352
L_20_03_06–42	0.519	0.011	0.0683	0.0011	0.65572	14.64129	0.2358041	0.05573	0.001	101%	833	91.1	146
L_20_03_06–43	3.032	0.069	0.2439	0.0044	0.70069	4.100041	0.07396548	0.0912	0.0017	100%	119.3	26.4	137.2
L_20_03_06–44	2.446	0.054	0.2194	0.0036	0.67619	4.557885	0.07478754	0.0816	0.0016	102%	183.9	45	205.8
L_20_03_06–45	1.798	0.041	0.1597	0.0034	0.83339	6.261741	0.133312	0.0826	0.0014	92%	712	100.4	455
L_20_03_06–46	1.37	0.13	0.1278	0.0025	0.52094	7.824726	0.1530658	0.0842	0.0088	93%	425	72.6	252
L_20_03_06–48	1.981	0.047	0.1906	0.0038	0.72878	5.24659	0.1046015	0.0758	0.0014	102%	146.8	46.1	175
L_20_03_06–49	1.982	0.051	0.1878	0.0034	0.7123	5.324814	0.09640238	0.0758	0.0016	100%	129.7	41.4	157
L_20_03_06–50	0.499	0.01	0.066	0.0011	0.67307	15.15152	0.2525253	0.05457	0.001	100%	683	175.9	240
L_20_03_06–51	2.166	0.066	0.2068	0.0041	0.54218	4.83559	0.09587001	0.0754	0.0021	104%	51.9	19.74	88.8
L_20_03_06–52	2.554	0.088	0.2015	0.004	0.4857	4.962779	0.09851671	0.0913	0.0029	93%	63.5	17.6	91.8
L_20_03_06–53	1.522	0.038	0.1492	0.0027	0.53192	6.702413	0.1212903	0.0737	0.0017	96%	195	71.5	243
L_20_03_06–54	1.676	0.042	0.1685	0.0028	0.49412	5.934718	0.09861846	0.0716	0.0017	101%	98.9	29.4	102.9
L_20_03_06–55	1.761	0.039	0.1749	0.0034	0.70902	5.717553	0.1111474	0.0721	0.0013	101%	392	39.3	142.6
L_20_03_06–56	0.495	0.01	0.065	0.0011	0.69659	15.38462	0.260355	0.0547	0.00097	100%	1094	238.6	328
L_20_03_06–57	2.632	0.056	0.2317	0.0044	0.76817	4.315926	0.08195975	0.0814	0.0014	103%	173.9	29.43	145.3
L_20_03_06–59	0.514	0.011	0.0652	0.0011	0.62726	15.33742	0.2587602	0.05692	0.0011	97%	871	310	458
L_20_03_06–60	0.492	0.011	0.0645	0.0011	0.66353	15.50388	0.2644072	0.0546	0.001	99%	682	207	278
L20_03_07–1	2.496	0.058	0.2187	0.0037	0.6814	4.572474	0.07735781	0.0831	0.0017	100%	157.4	29.4	131.6
L20_03_07–2	0.473	0.013	0.0624	0.0014	0.75716	16.02564	0.3595496	0.05476	0.0012	99%	1006	319	387
L20_03_07–4	2.243	0.055	0.185	0.0052	0.83151	5.405405	0.1519357	0.0884	0.0017	92%	560	110	408
L20_03_07–5	0.536	0.012	0.0655	0.0012	0.76289	15.26718	0.279704	0.05949	0.0011	94%	934	204	314
L20_03_07–6	0.56	0.02	0.0675	0.0015	0.43582	14.81481	0.3292181	0.0596	0.0019	94%	701	215	317
L20_03_07–7	0.508	0.01	0.0662	0.0012	0.61615	15.10574	0.2738201	0.05572	0.0011	99%	865	138.7	197.1
L20_03_07–8	1.77	0.034	0.1745	0.003	0.71323	5.730659	0.09852136	0.0737	0.0013	100%	345	74.8	272.3
L20_03_07–9	1.657	0.038	0.1641	0.0028	0.63438	6.093845	0.1039779	0.0734	0.0016	99%	245.5	27.79	109
L20_03_07–10	1.066	0.03	0.1104	0.0027	0.83314	9.057971	0.2215265	0.07	0.0014	92%	1220	108.6	301
L20_03_07–11	2.46	0.094	0.2072	0.0062	0.90394	4.826255	0.144415	0.0855	0.0017	97%	880	107.9	663
L20_03_07–12	0.738	0.032	0.0848	0.0022	0.5876	11.79245	0.3059363	0.063	0.0023	94%	676	539	913
L20_03_07–13	2.128	0.064	0.2059	0.006	0.85586	4.856727	0.1415268	0.075	0.0015	105%	900	69	245
L20_03_07–14	0.514	0.012	0.0676	0.0012	0.58602	14.7929	0.2625958	0.0551	0.0013	101%	450	118.8	184
L20_03_07–15	0.555	0.012	0.0692	0.0012	0.69342	14.45087	0.2505931	0.05804	0.0011	97%	782	125.3	202.2
L20_03_07–16	0.556	0.012	0.0719	0.0012	0.73049	13.90821	0.2321258	0.05628	0.0011	100%	612	42.5	67.5
L20_03_07–17	2.051	0.046	0.1916	0.0035	0.65776	5.219207	0.09534041	0.0774	0.0015	100%	243	97.3	371
L20_03_07–18	0.528	0.011	0.0651	0.0011	0.63608	15.36098	0.2595558	0.05896	0.0012	95%	886	97.5	163.2
L20_03_07–19	2.086	0.06	0.1912	0.0047	0.78752	5.230126	0.1285648	0.079	0.0017	99%	391	113.2	453
L20_03_07–20	1.776	0.044	0.177	0.0037	0.76257	5.649718	0.1181014	0.0732	0.0014	101%	420	51.7	172
L20_03_07–21	2.228	0.053	0.2077	0.0039	0.73216	4.814636	0.09040483	0.0776	0.0015	103%	297	142.4	568
L20_03_07–22	2.301	0.07	0.2098	0.005	0.76548	4.766444	0.113595	0.0794	0.0018	102%	161	56.5	237
L20_03_07–23	0.731	0.016	0.0904	0.0016	0.73798	11.06195	0.1957867	0.05867	0.0011	100%	546	214	391
L20_03_07–24	1.785	0.043	0.1694	0.0034	0.76139	5.903188	0.1184819	0.0765	0.0015	97%	303.9	100.3	382.4
L20_03_07–25	3.112	0.079	0.2425	0.0046	0.38859	4.123711	0.07822298	0.0935	0.0025	98%	63.6	68.2	341
L20_03_07–26	13.93	0.29	0.5363	0.0096	0.67825	1.864628	0.03337764	0.1887	0.0037	101%	46.5	21.75	220.7
L20_03_07–27	2.417	0.094	0.1954	0.005	0.48888	5.117707	0.1309546	0.0892	0.0031	93%	82.8	19.72	108.6
L20_03_07–28	0.511	0.013	0.0668	0.0012	0.53669	14.97006	0.2689232	0.0554	0.0013	100%	425	119.3	175
L20_03_07–30	0.503	0.011	0.0636	0.0011	0.61352	15.72327	0.2719434	0.05726	0.0012	96%	917	110.3	169.9
L20_03_07–31	0.509	0.011	0.0666	0.0012	0.55199	15.01502	0.2705408	0.056	0.0013	100%	591	151	226

(*continued on next page*)

Table 2 (*continued*)

Spot	207 Pb/ 235U	2SE (abs)	206 Pb/ 238U	2SE (abs)	Rho	238U/ 206 Pb	2SE (abs)	207Pb/ 206 Pb	2SE (abs)	% conc	[U] (μg g-1)	[Th] (μg g-1)	[Pb] (μg g-1)
L20_03_07–32	2.823	0.055	0.2327	0.0038	0.66855	4.297379	0.07017636	0.0881	0.0017	99%	170	89.2	422
L20_03_07–33	0.511	0.011	0.0674	0.0011	0.64463	14.8368	0.2421435	0.05503	0.0011	101%	659	88.6	125.3
L20_03_07–34	0.567	0.034	0.0698	0.0019	0.54115	14.32665	0.3899804	0.0577	0.0026	95%	568.9	114.5	182
L20_03_07–35	1.03	0.027	0.1203	0.0023	0.65397	8.312552	0.1589266	0.0622	0.0014	102%	232	152.9	370.8
L20_03_07–36	1.908	0.04	0.1855	0.003	0.63001	5.390836	0.08718332	0.0745	0.0015	101%	153.5	30.74	117.3
L20_03_07–40	4.909	0.093	0.3356	0.0058	0.74461	2.979738	0.05149726	0.1065	0.0019	103%	166.9	49.2	338
L20_03_07–41	0.4826	0.0095	0.0634	0.0011	0.72329	15.77287	0.2736618	0.05529	0.001	99%	989	127.8	176

crystals. Furthermore, rounded zircons with aspect ratios of 1:1 and sizes from 80 to 90 μm are also found. In this case, internal structures are more difficult to see, since most of them are faint even though some inherited cores were distinguished. In general, recrystallized rims were not identified and in the few analyzed cases, they did not give good results.

The predominant age provenance in the sample corresponds to the youngest peak on the probability density plot at late Silurian–Middle Devonian (30% of the sample), being the main age of 415 Ma. Moreover, other groups of important ages found in the sample are Meso-proterozoic between 1000 and 1400 Ma, accounting for 44% of the analyzed zircons, and Neo-proterozoic making up the 11% of the sample. Isolated ages at ca. 1800 and 2700 Ma. represent the oldest provenance ages in the sample. Also, early Cambrian ages are present in this sample (Fig. 6).

In order to estimate the maximum depositional age of the protolith of this sample, recommendations and methods of Dickinson and Gehrels (2009) were used. Considering the weighted mean of the three youngest zircon dates, an age of 392.1 ± 3.9 Ma was calculated (Fig. 6). This age agrees with the youngest single grain age of 389.8 ± 6 Ma, being the maximum depositional age Middle Devonian.

3.2. Metamorphism

The metamorphism of the Paleozoic rocks of Cuesta del Rahue area was developed under low-grade conditions. The phyllitic rocks present a well-developed lepidoblastic texture defined by the presence of fine flakes of chlorite, muscovite, and biotite (Fig. 7). In these rocks, porphyroblasts of opaque minerals are common with strain shadows of quartz. In the metasandstones, subhedral porphyroblasts of biotite were found surrounded by the main foliation (S_1), so they can be interpreted as pre-tectonic porphyroblasts that would represent a previous thermal event affecting the sedimentary protolith. Also, it is common to find evidence of a later thermal event (contact metamorphism) overprinting the main metamorphic fabric (S_1) as spots of very fine-grained chlorite and sericite. In addition, in some cases post-tectonic porphyroblasts of muscovite are found overprinting the main foliation of the samples.

In terms of regional metamorphic events, a low to intermediate P-T event is described near Piedra Santa with the presence of andalusite and cordierite porphyroblasts (Franzese, 1995). Furthermore, a contact metamorphic event is described for the Piedra Santa Complex similar to the one described in the Cuesta del Rahue area (Franzese, 1995). Nevertheless, the presence of porphyroblasts of cordierite and andalusite as well as spotted schists in the Piedra Santa Complex indicates that they were formed in the inner part of a contact aureole, closer to the heat source.

K–Ar ages were calculated on the fine fraction of schists in the Piedra Santa Complex by Franzese (1995), obtaining imprecise ages from Middle Devonian to late Carboniferous (372 ± 18 to 311 ± 16 Ma) for the regional metamorphism, while the contact metamorphic event would be late Carboniferous–early Permian (299 ± 14 Ma), which is probably related to the emplacement of the Chachil Plutonic Complex.

Taking into account the age of the detrital zircons of this work (389.8 ± 6 Ma) and the age of the granite that cuts the regional cleavage in the Piedra Santa area, ca. 357 Ma according to Rapela et al. (2022) (Table 1), the Franzese's ages for the regional metamorphism can be pinpointed between the Late Devonian and the earliest Carboniferous.

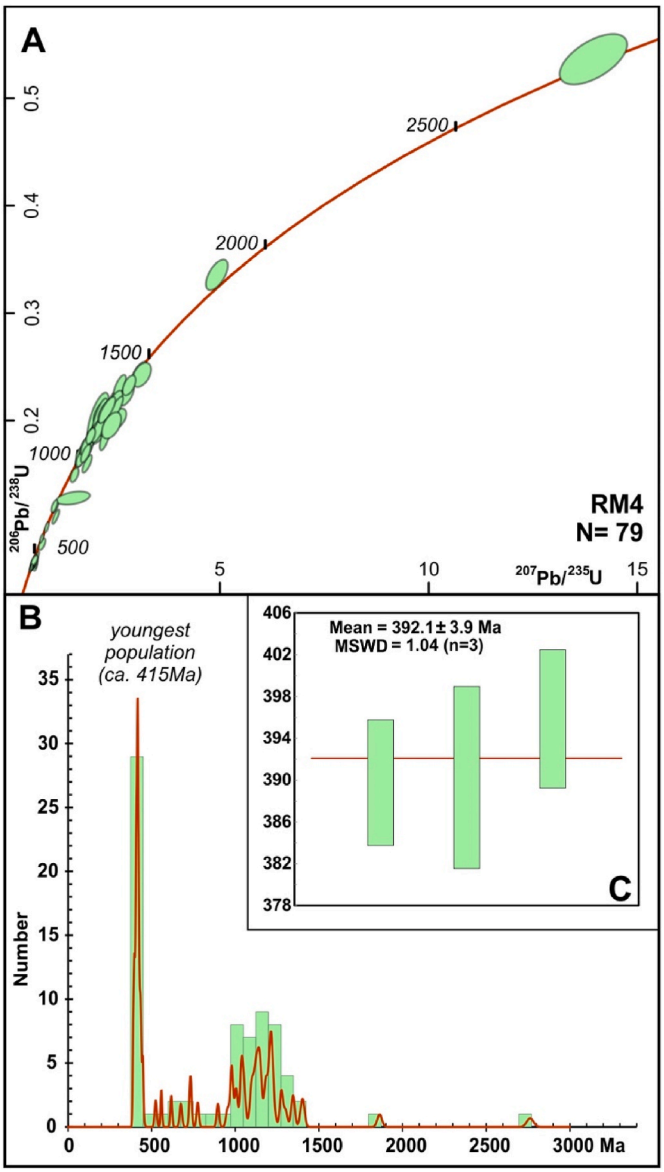

Fig. 6. (A) Concordia diagram and (B) frequency histogram for analyzed zircons from sample RM4. (C) Weighted mean age for the three youngest concordant zircons.

3.3. Plutonic rocks

Two different types of plutonic rocks can be found in the study area

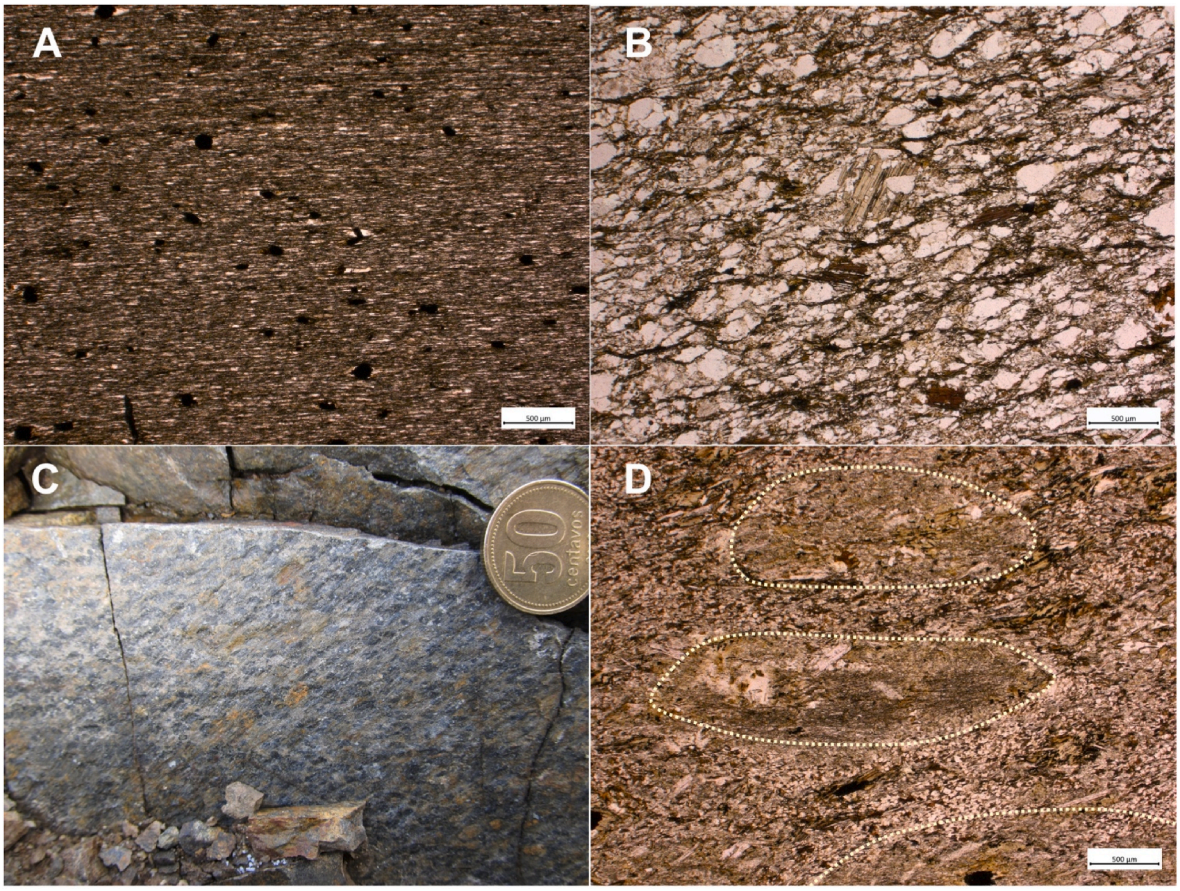

Fig. 7. Photomicrographs and field photographs of the metasedimentary rocks. (A) Photomicrograph of a slate with porphyroblasts of opaque minerals and pervasive S_1 Chanic foliation. (B) Photomicrograph of a metasandstone with rough cleavage and biotite porphyroblasts. (C) Field photograph of a spotted slate. (D) Photomicrograph of a spotted metasedimentary rock. Yellow dashed lines mark the spots of very fine-grained chlorite, sericite, and graphite.

(Fig. 8A and B), both cutting the Paleozoic structures. The first one corresponds to leucogranitic dikes that intruded the metasedimentary sequence with sharp contacts, crosscutting the tectonic foliation of the metamorphic rocks (Figs. 8B, 11 and 12). These igneous rocks have equigranular medium-grained texture with abundant quartz, plagioclase, and K-feldspar (Fig. 8C). Fine flakes of biotite are sporadically present but in subordinate modal proportions. It is common to find perthites in K-feldspar as well as myrmekite lobes in the contacts between quartz and feldspars. Also, graphic texture in quartz is sometimes present. These dikes were dated by Hervé et al. (2018) at 306 ± 2 Ma (late Carboniferous) (Table 1) and in some cases are deformed by Gondwanan thrusts and folds.

Secondly, a pluton of granodioritic composition (Figs. 2 and 8A) assigned to the Chachil Plutonic Complex (Leanza, 1992), is found to the south of the Cuesta del Rahue area). These rocks are light gray with an equigranular coarse-grained texture defined by the presence of abundant quartz, plagioclase, and biotite. K-feldspar is also present, but it is found in low proportions (Fig. 8D). Zircon and apatite commonly appear as accessory minerals. Moreover, secondary chlorite, epidote, and prehnite replace biotite, and plagioclase is commonly zoned with dirty cores replaced by sericite and pristine rims. The age of the Chachil Plutonic Complex is late Carboniferous to early Permian (Sillitoe, 1977; Varela et al., 1994; Hervé et al., 2018; Romero et al., 2020; Table 1). This plutonic rock crosscuts all the Paleozoic structures (Chanic and Gondwanan) of the Cuesta del Rahue area. The late Carboniferous to early Permian ages of these igneous rocks indicate their possible relationship with the magmatism of the final stages of the Gondwanan orogenic cycle (in the sense of Heredia et al., 2016).

3.4. Structures

3.4.1. Paleozoic structures

The cross section along the road RP-46 in the Cuesta del Rahue (Fig. 9A) shows a rather homoclinal sequence of low-grade metasedimentary rocks with an average dip of 35°–40° toward the N to NNE. An exception is found at the lowermost part of the section, where lower grade phyllites appear with subvertical attitude in the footwall of a thrust. All the metasedimentary rocks cropping out in the Cuesta del Rahue section are affected by a tectonic foliation (S_1, Fig. 7) that has a very low angle with the stratification planes. The dipping of the S_1 is nevertheless lower than the dipping of the bedding in all the locations where both surfaces are clearly recognized (Fig. 10A and B). The polarity of the sedimentary succession being normal (see Section 3.1.1), all the Cuesta del Rahue section belongs to a tilted normal limb of a hm- or km-scale asymmetric fold, whose hinge zone would be located further north. If we restore the later tilting, the vergence of this fold would be NNE to NE.

As mentioned in Section 3.3, the metasedimentary rocks and their foliation are cut by several leucogranitic dikes (more abundant at the base of the section). The age of the deformation related to the S_1 foliation is then constrained between the age of the protolith of the metasedimentary rocks (389.8 ± 6 Ma; this work) and the age of the leucogranitic dikes (306 ± 2 Ma; Hervé et al., 2018), which is a clear indicator that this deformation is related to the Chanic orogeny, Late Devonian–early Carboniferous in age.

The homoclinal attitude of the bedding in the Cuesta del Rahue section is only disrupted by some brittle thrusts and asymmetric open folds at various scales (Fig. 2). These structures affect the S_1 cleavage

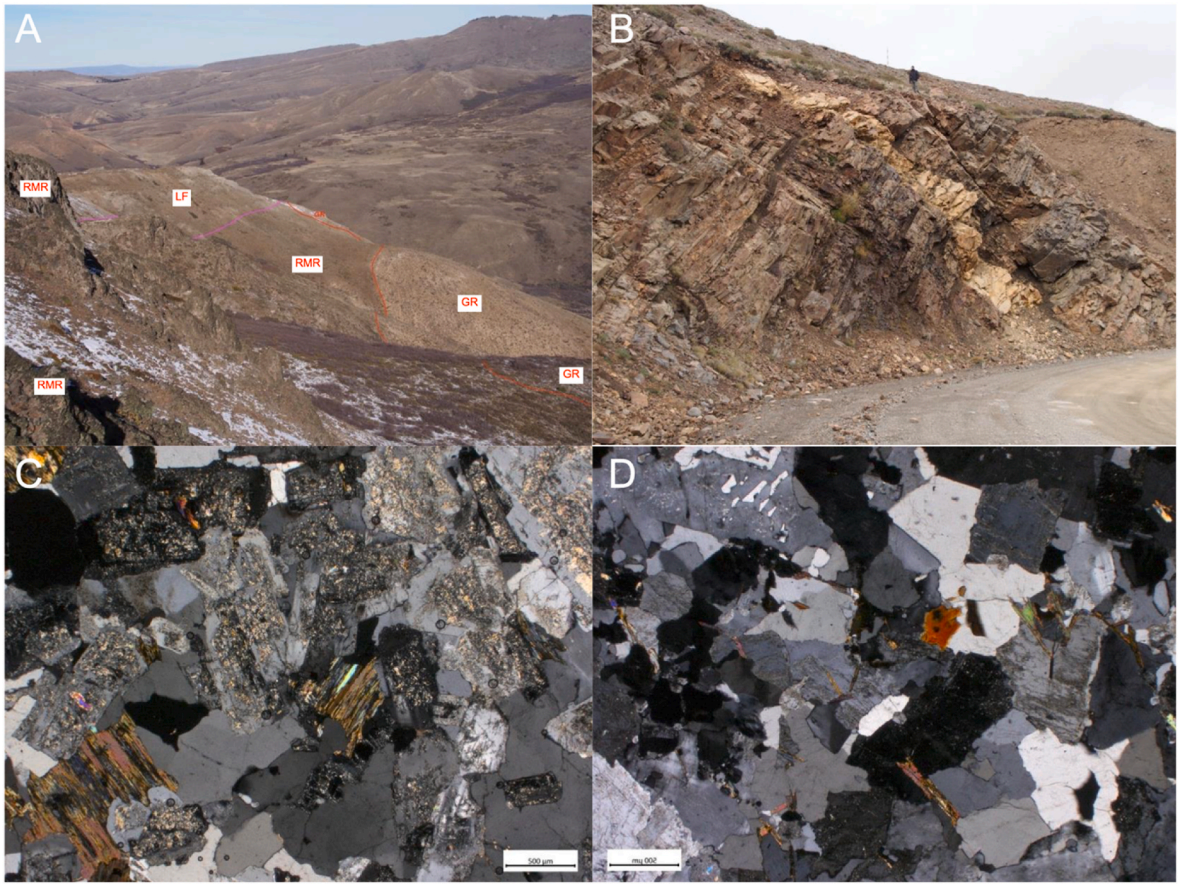

Fig. 8. Field photographs and microphotographs of Paleozoic plutonic rocks: (A) Granodioritic pluton (GR) related to the Chachil Plutonic complex (late Carboniferous-early Permian), which intrudes the Paleozoic rocks of Cuesta del Rahue (RMR) and is unconformably covered by the La Lapa Formation (Late Triassic) (LF). (B) Late Carboniferous leucogranitic dikes intruding the Cuesta del Rahue Paleozoic rocks. (C) Photomicrograph of the main mineral assemblage and texture of the granodioritic pluton. (D) Photomicrograph of common microstructures and texture of the leucogranitic dikes.

and the late Carboniferous leucogranitic dikes (Fig. 10E) and were generated under non-metamorphic conditions in later deformation events. Looking at the section with north to the left, the minor folds show a generalized open "Z" asymmetry, with their axial planes dipping toward the south or subvertical (Fig. 10B). The folds with a more vertical axial plane have axis plunging between 5° and 25° to the WSW and could have been formed during the folding of the tight Chanic fold by large cartographic-scale folds with NW–SE axial traces (Fig. 9B). These NW–SE cartographic-scale folds must be related to the subsequent Gondwanan orogeny, developed in late Carboniferous–early Permian times, since they do not affect the Mesozoic rocks of the Cuesta del Rahue area (Fig. 2). Most of the minor "Z" folds, however, are open, with the axial planes more inclined toward the south and usually marked by joints or even normal faults with small displacements. These structures are clearly extensional, affect Gondwanan thrusts planes and must be related with the beginning of the Andean orogenic cycle (described in next Section).

The late Carboniferous leucogranitic dikes of the Cuesta del Rahue section are affected by ~ S-directed reverse faults that we also interpret as Gondwanan. They essentially follow the stratification planes of the hosting sequence (Fig. 10C), suggesting a flexural slip deformation mechanism (Fig. 11) that is compatible with the development of the large-scale anticline (hinge zone toward the ~S) that tilts the Chanic normal limb (Fig. 9B). In the northern part of the Cuesta del Rahue area and also in the southwestern part of the Piedra Santa area, the Gondwanan thrusts have NNE-dipping planes (Fig. 10E), while in the lowest part of the Cuesta del Rahue road section the main Gondwanan thrust dips to the N. There, a large Gondwanan thrust (dipping 22° toward 350°) places the whole section of north-dipping rocks on top of lower-grade phyllites with subvertical bedding (Fig. 10C). The deformation band of this thrust is cataclastic and is several decimeters thick, with a thin fault gouge at the base and riedel structures on top (Fig. 10D). These structures and some drag folds in the footwall indicate tectonic transport direction broadly to the south. This gently dipping thrust is in turn affected by a subvertical reverse Andean fault and, some meters to the south, also by a north-directed, and brittle thrust with metric displacement, which we also interpret as Gondwanan (Figs. 10C and 13B).

3.4.2. *Andean structures*

The open minor folds with "Z" asymmetry (looking the outcrops with the north to the left) and more gently south-dipping axial planes, affect the Gondwanan flexural sliding surfaces that are in turn crosscutting the late Carboniferous dikes (Fig. 11). Along the Cuesta del Rahue section the axis of these folds are oriented toward the WNW, with an average plunge of less than 20°. However, to the north of the section, the axes are slightly rotated (10°–15° clockwise) and the average plunge increases to near 40°. The axial planes are commonly marked by a locally intense jointing (Fig. 9A) that in some cases evolve to normal faults with cm-to m-size displacements. All these observations point to an extensional mechanism for the formation of these folds, in some cases showing clear kink-band geometries, which would be related to the Mesozoic extensional event that constitutes the pre-orogenic stage of the Andean cycle. Normal fault surfaces that could be measured show dips of 30°–55° toward the SSW (e.g. Figs. 11 and 12A), although conjugate normal faults dipping toward the NNE (Fig. 12B) are also identified in the Cuesta del Rahue structural section (Fig. 9A). Therefore, the direction of the main

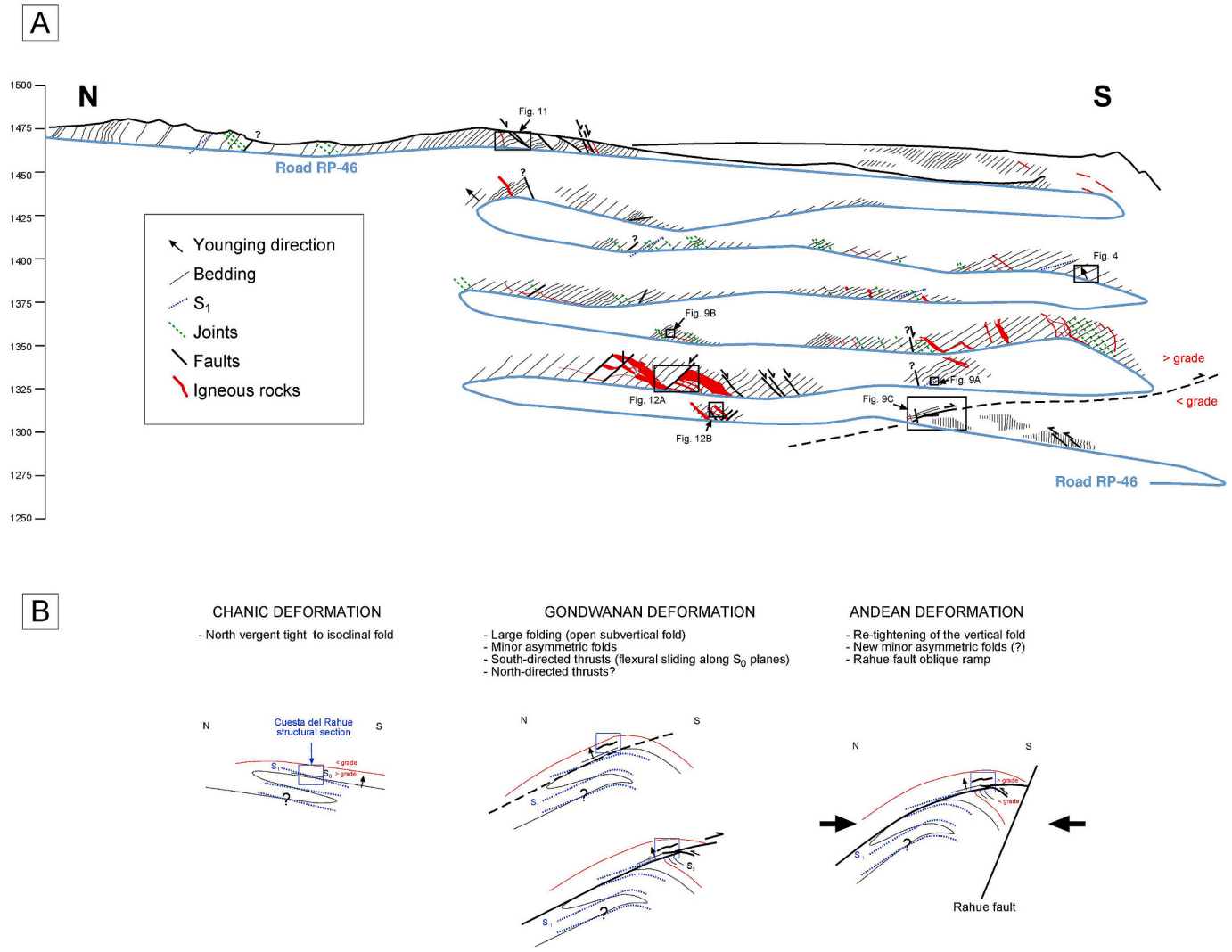

Fig. 9. (A) Schematic interpretation of the Cuesta del Rahue structural section along road RP-46 (blue line), projected in a N–S section. (B) Interpreted evolution through the Chanic, Gondwanan and Andean contractional deformations. The Chanic fold forms part of the large normal limb of the asymmetric fold represented in Fig. 14, which occupies most of the Cuesta del Rahue area.

extensional stresses would be NNE–SSW, in accordance with the orientation of the axis of the extensional folds. This orientation is also coherent with the general extensional direction in the Mesozoic Neuquen Basin located to the NE (e.g., Bechis et al., 2014).

In general, the contractional structures related to the Andean orogeny are poorly developed within the basement of the study area (Fig. 13B), where they mainly produce the fracture, rotation, and tightening of the Paleozoic structures. However, they are clear in the borders of the Paleozoic massif, where they affect the Mesozoic–Cenozoic cover (Fig. 2). The structures related to this orogenic stage affecting the Mesozoic–Cenozoic cover, are part of the Aluminé Fold and Thrust Belt (ALFTB) (Fig. 1B), which extends over the cordilleran and precordilleran zones between 38°30' and 40°30' S latitude. The Andean orogeny is also responsible for the current relief of the area (Fig. 13A).

The main Andean structure of the study area is the NW–SE Rahue oblique ramp fault, which links the N–S Catan Lil back-thrust with the E–W Piedra Santa fault, a large tear fault of the ALFTB that partially reactivated the Huincul lineament (Fig. 1C). The Rahue fault was limiting a Mesozoic hemigraben developed toward the NE (García Morabito and Ramos, 2012) and was later inverted during the Andean orogeny, superimposing the Paleozoic metamorphic rocks of the Cuesta del Rahue area on different lithostratigraphic units of the Mesozoic–Cenozoic Andean cover (Fig. 2). The slight counter-clockwise rotation (10°–15°) of the Andean extensional fold axes and also of the trend of the Gondwanan thrusts takes place toward the Rahue fault, suggesting that this rotation occurred during the Andean orogeny.

4. Correlations and tectonostratigraphic context

The Paleozoic rocks of Cuesta del Rahue area have a very similar lithological composition to the ones from the Carrizalito range (Figs. 1B and 16) and the westernmost part of the Piedra Santa range located farther east (Figs. 14 and 15), though the latter exhibit a higher metamorphic grade. In most of the Piedra Santa area, the maximum sedimentation ages do not seem to exceed the Late Ordovician (Romero et al., 2020), while in the Cuesta del Rahue area they range between the Middle Devonian (this study) and the Late Devonian (Ramos et al., 2010) (Table 1). Besides, the structures and cleavages associated with the first deformation of these rocks appear, in both cases, cut by early to late Carboniferous granitoids, indicating that such deformation is mainly pre-Carboniferous. In addition, the study of the metamorphism in Piedra Santa by Franzese (1995) (Table 1) and the metamorphism described in this work for the Cuesta del Rahue (see chapter 3.2), suggest the occurrence of a common regional syn-kinematic metamorphic event between the Late Devonian and the early Carboniferous (Fig. 15).

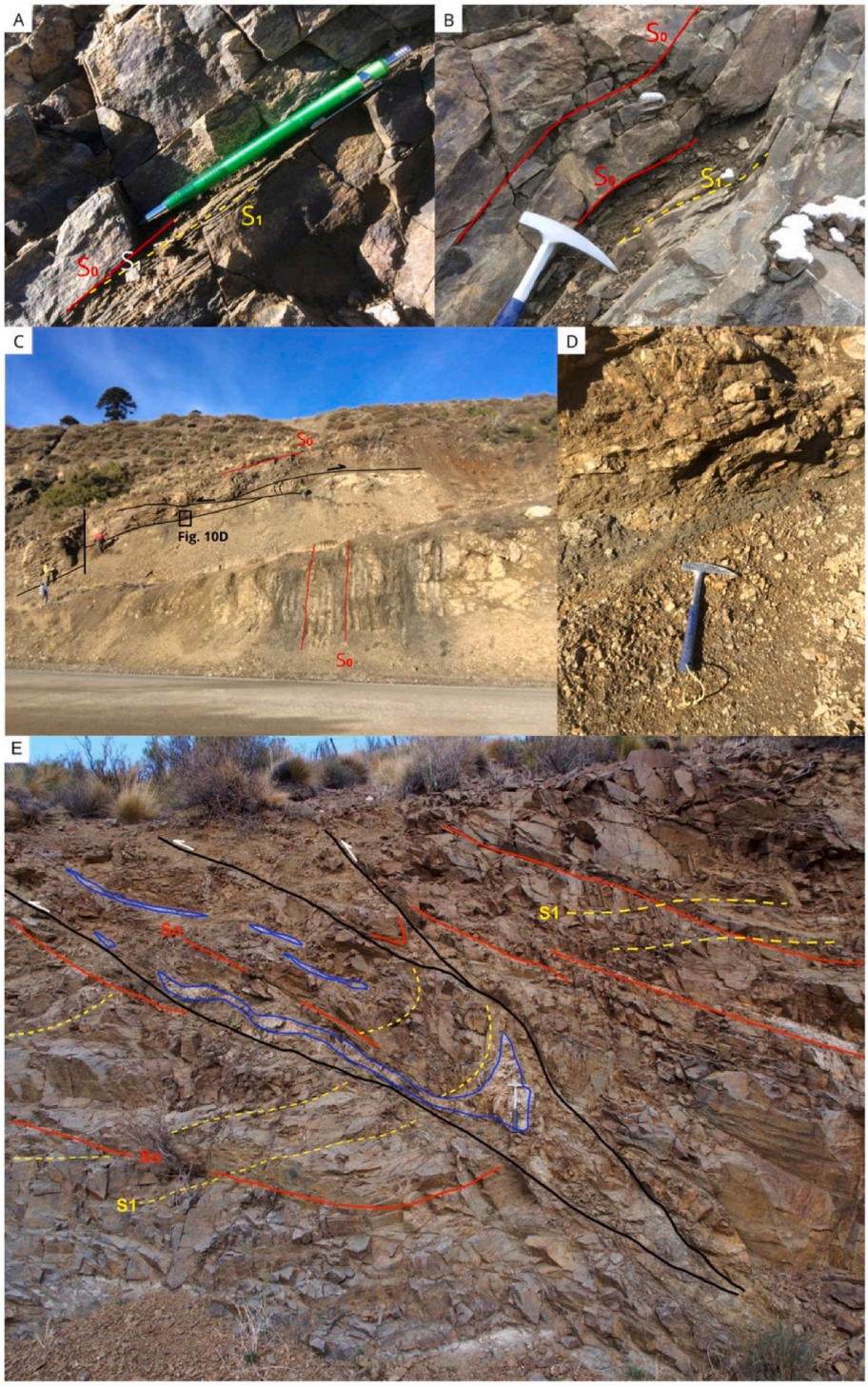

Fig. 10. Field examples of Paleozoic structures along the road RP-46 in the Cuesta del Rahue (Cuesta del Rahue section). North is to the left in all the photos, except (D). (A) Relationship between the bedding (S_0) and the Chanic foliation (S_1). (B) Late minor fold affecting both the S_0 and the S_1. (C) ~S-directed thrust at the base of the Rahue section affected by a ~N-directed thrust, both interpreted as Gondwanan structures. (D) Detail of the fault damage zone related to the south-directed thrust in C. (E) Brittle Gondwanan thrusts with SSW tectonic transport affecting late Carboniferous leucogranitic dikes and the S_1 Chanic foliation. North to the right.

In nearby areas, located southwards of the Huincul lineament (Patagonian Sector of the Paleozoic basement of the Andes), Serra--Varela et al. (2019, 2022) recognized a pre-Wenlock deformation (middle Silurian), during which high grade metamorphic conditions were reached, bearing no apparent consequences for the rocks of Piedra Santa-Rahue (Fig. 15). Furthermore, these authors indicated the presence of a great amount of plutonic arc rocks that, though they formed between the Silurian–Devonian boundary (Loske et al., 1999) and the earliest late Carboniferous (I-type granitoids, Pankhurst et al., 2006), they reached their maximum development during the Devonian (Fig. 15). These Devonian and Carboniferous arc-related igneous rocks are not present in the study area. Xenoliths of the early Paleozoic metamorphic rocks (Serra-Varela et al., 2019) appear inside the Devonian plutonic rocks. Serra-Varela et al. (2021) included these metamorphic rocks in the Colohuincul Complex, whose sedimentation age would be mainly early Paleozoic (Ordovician and older). Finally, these last authors described a deformation event mainly between the Late Devonian and the early Carboniferous, which would be related to the same subduction process that gave rise to the magmatic arc (Gondwanan subduction orogen). This deformation process took place before the one associated with a continental collision (Gondwana collisional orogen), which was developed between the late Carboniferous and early Permian

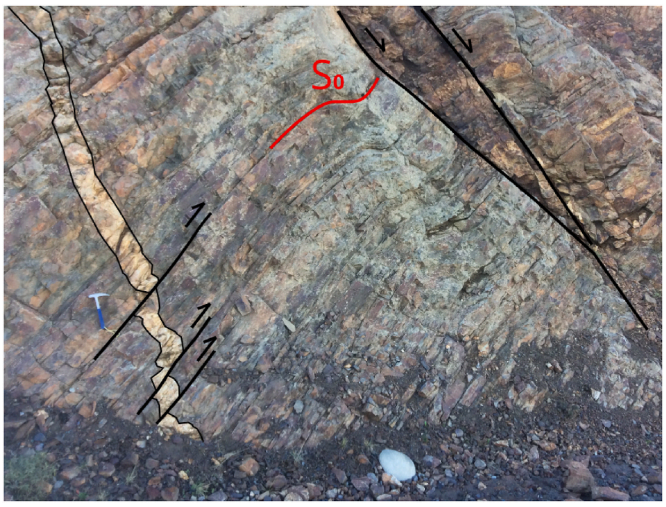

Fig. 11. Flexural slip related to the development of Gondwanan folds in the Cuesta del Rahue section. In black, normal faults related to the Mesozoic pre-orogenic stage of the Andean cycle. North to the right.

(Fig. 15) with the formation of some syn-orogenic granitoids (S-type granitoids, Pankhurst et al., 2006). Although this subduction orogen of the North Patagonian Andes seem to be of similar age to the first deformation event of the Rahue-Piedra Santa Paleozoic rocks, here this deformation predates the intrusions of ca. 357 Ma, therefore reaching only the lowest part of the early Carboniferous. On the contrary, in the North Patagonian Cordillera, this pre-collisional deformation seems to have reached the earliest late Carboniferous (Serra-Varela et al., 2022), (Fig. 15). Moreover, as is usual in subduction-related orogens outside the accretionary prism, this pre-collisional Gondwanan Patagonian deformation would only reach certain metamorphic conditions in the nearby areas of the magmatic arc, where it could develop a slightly penetrative cleavage, showing a general vergence toward the E, very different to the one exhibited by the Gondwanan structures in the study area (SSW).

However, north of the Huincul lineament (Cuyo Sector of the Andean basement), the Paleozoic rocks are similar in age and composition, as well as in the type and age of deformation, to those of the study area. These rocks show no evidence of a tectonic event in the early Paleozoic, as described by Serra-Varela et al. (2022) southwards of the Huincul lineament, so there are no significant unconformities in the pre-Late Devonian sedimentary sequence (Fig. 15).

Thus, in the Cordillera del Viento (37°S) (Figs. 1B and 16), Giacosa et al. (2014) described the Guaraco Norte Formation (Zappettini et al., 1987) as a metamorphized sandy-pelitic succession that reached the Late Devonian (maximum depositional age of ca. 374 Ma) according to Zappettini et al. (2012). These rocks have a very intense deformation that originated two pervasive tectonic foliations and ductile faulting and that is very similar to the Piedra Santa deformation (Fig. 14). The Guaraco Norte Formation would be unconformably covered by the Arroyo del Torreón Formation. The Arroyo del Torreón Formation is composed of volcanic and sedimentary rocks, deformed under non-metamorphic to very low-grade metamorphic conditions during the Gondwanan orogeny (late Carboniferous–early Permian). In a volcanic rock, interbedded in the basal part of this lithostratigraphic unit, Suárez et al. (2008) obtained zircon ages of 328 ± 2 Ma (Serpukhovian, late early Carboniferous). Based on this age, the Arroyo del Torreón and overlying Huaraco Formation could be correlated with the lower section of the Paganzo Group (Limarino et al., 2006) of the northern part of the Cuyo Sector (Fig. 15). This implies that the deformation of the Guaraco Norte Formation occurred between the Late Devonian and the Serpukhovian (Fig. 15). Giacosa et al. (2014) correlated this formation with the pre-orogenic succession of the Chanic cycle and the Arroyo del

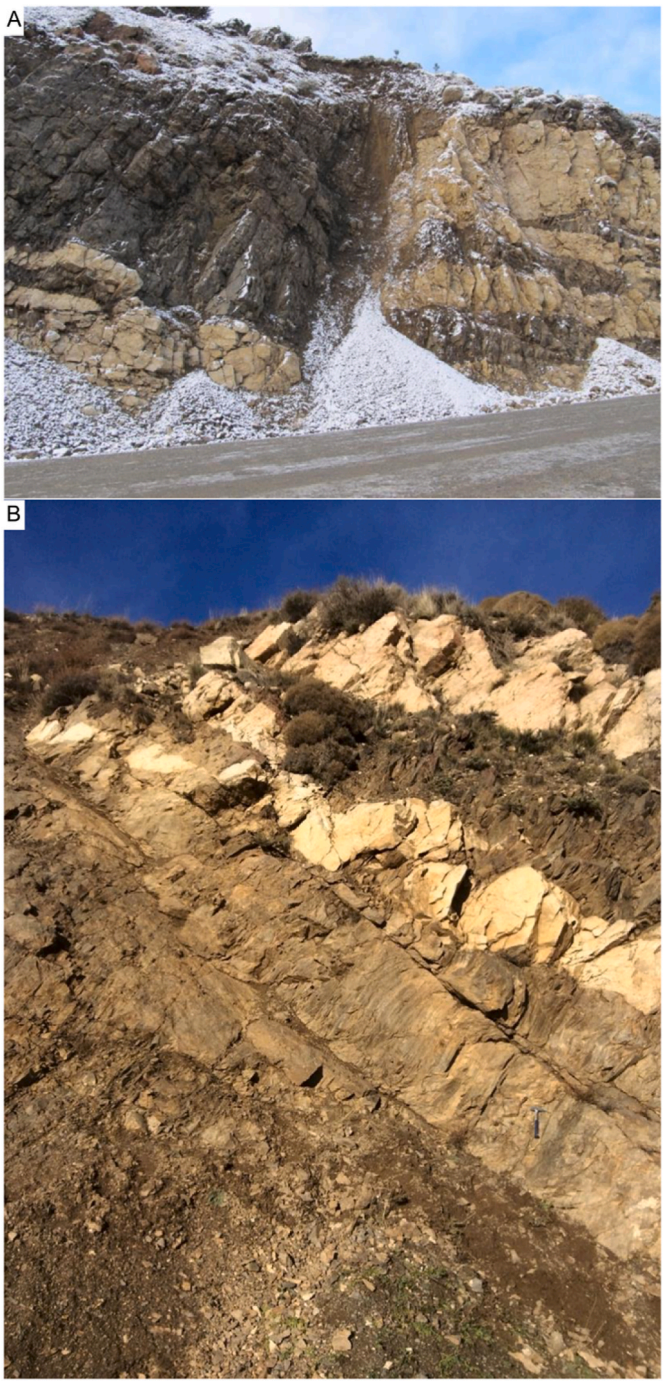

Fig. 12. Photographs of Andean extensional structures in the Cuesta del Rahue section. (A) Normal fault affecting late Carboniferous dikes. North to the left. (B) Normal faults and related folds affecting pre-Carboniferous metasedimentary rocks and late Carboniferous dikes. North to the left.

Torreón and Huaraco formations with the pre-orogenic succession of the Gondwanan cycle.

Farther north, in the Sierra de Guarguaraz (Frontal Cordillera, 35°S; Figs. 1B and 16), García-Sansegundo et al. (2016) described the deformation that affects the hinterland of the Chanic orogen (Guarguaraz Complex), formed by a metasedimentary sequence with Ediacaran (López de Azarevich et al., 2009), early Cambrian (maximum depositional age of ca. 530 Ma, according to López and Gregori, 2004), and Devonian ages (García-Sansegundo et al., 2016). The Devonian rocks are the Vallecitos beds (Heredia et al., 2012) which also crop out in the

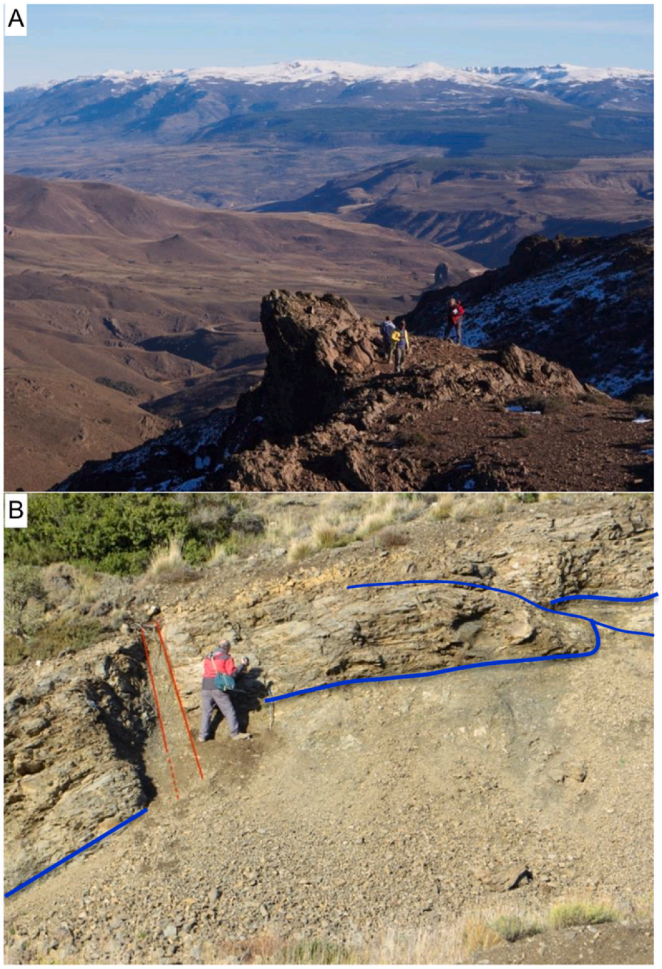

Fig. 13. Photographs of Andean compressional structures in the Cuesta del Rahue section. A) Relief produced on the hangingwall of the Rahue fault, where the Paleozoic rocks crop out (geologists working on them). The Rahue fault runs along the river valley. The sunny slope is formed by the Cenozoic volcanic rocks of the footwall. South to the right. B) Steeply-dipping north-directed Andean reverse fault. The red lines bound the damage zone (with fault gouges) of this fault. The blue lines indicate the location of the Gondwanan thrusts of Fig. 10E. North to the left.

Carrizalito and El Plata ranges (Figs. 1B and 16). They are similar to the Cuesta del Rahue beds, although the absence of conglomerates in the Vallecitos beds would indicate that they are more distal turbidite sequences. The Guarguaraz Complex is mainly composed of siliciclastic rocks with Cambrian limestone lenses in the basal part and volcanic and subvolcanic basic igneous intercalations of pre-Devonian ages (Ediacaran to Silurian) (López and Gregori, 2004; Davis et al., 1999). This complex is affected by a high pressure and low temperature metamorphism (HP-LT metamorphism), mainly developed in Middle Devonian times (ca. 390 Ma, Willner et al., 2011), which is associated with a Devonian subduction event (Fig. 15), developed prior to the Chanic collision in Late Devonian times (Ramos et al., 1986; Davis et al., 2000; Heredia et al., 2012, 2016, 2018a, 2018b). This subduction event only affected the southern Cuyo Sector, where the Chilenia and Cuyania subplates were separated by a small ocean (Fig. 16). Toward the end of the subduction and during the Chanic collision (starting at ca. 377 The Guaraco Norte Formation would eventually be unconformably covered by the Arroyo del Torreón Formation 374 Ma, Davis et al., 1999; Heredia et al., 2016) the Guarguaraz Complex deformation took place under low pressure/intermediate-high temperature (LP/IT-HT metamorphism) conditions, allowing the exhumation of high pressure rocks from the subduction zone (García-Sansegundo et al., 2016; Heredia et al., 2016). This collision almost completely erased the previous HP/LT subduction event, which is indicated by a relict high-pressure cleavage, marked by the presence of Si-rich phengite (Massonne and Calderón, 2008) in albite and garnet blasts (Willner et al., 2011; García-Sansegundo et al., 2016). In this area, the main structures of the Chanic collisional orogeny are folds and ductile thrusts with up to two related cleavages and a clear vergence toward the west (Fig. 14). The Chanic deformation does not affect the El Plata Formation (García-Sansegundo et al., 2016) mainly deposited in late Carboniferous times, which can be correlated with the lower section of the Paganzo Group, in the sense of Limarino et al. (2006) (Fig. 15).

In the Cordón del Carrizalito (Andean Frontal Cordillera, 34°S; Figs. 1B and 16), García-Sansegundo et al. (2014) describe the Chanic deformation that affected the Late Ordovician Las Lagunitas Formation (Ticky et al., 2009) and the Vallecitos beds, which can reach the Devonian (Heredia et al., 2012). These sedimentary formations were intruded by subduction-related plutons (413 ± 2 to 389 ± 3 Ma) according to Dahlquist et al. (2018), which would be related to the Chanic subduction, according to García-Sansegundo et al. (2014). This magmatism could be the source of the ca. 415 Ma peak obtained from detrital zircons from the Cuesta del Rahue area. In the Cordón del Carrizalito area, the structures that affected the Ordovician–Devonian rocks were exclusively produced during the Chanic collisional event, mainly being west-vergent folds that show kilometer-scale overturned and normal limbs with an associated cleavage (Fig. 14). Also, some west-directed thrusts can be observed, which were developed at the brittle-ductile transition. These structures do not seem to affect the Carboniferous rocks equivalent to the El Plata Formation (Caminos, 1965), late Carboniferous in age (Folguera et al., 2003; Limarino et al., 2006) and equivalent to the lower Paganzo Group (Fig. 15). In this area, on the normal and subhorizontal limbs of the large Chanic folds, east-vergent folds with an associated rough cleavage appear (Fig. 14). These last structures have been interpreted by García-Sansegundo et al. (2014) as Gondwanan structures of late Carboniferous–early Permian age. These folds could be equivalent to the ENE–WSW kilometer-scale folds of the Cuesta del Rahue area, which also deform a large normal Chanic limb, although here the Gondwanan folds do not develop cleavage.

Finally, in the westernmost part of the Precordillera Cuyana, at the San Juan river section (31° S, San Juan province) (Fig. 16), Colombo et al. (2014) described Chanic syn-orogenic deposits that unconformably cover the El Codo Formation, of Middle–Late Devonian age (Amenábar and di Pasquo, 2008). These deposits belong to the Del Ratón Formation (Azcuy et al., 1981) from the Angualasto Group (in the sense of Limarino et al., 2006) (Fig. 15). The conglomeratic lower part of the Del Ratón Formation was probably deposited in a fjord zone, considering the abundance of glacial signs in these deposits, while the upper part was deposited near the coastline by a system of fan deltas (Colombo et al., 2014). The conglomeratic deposits located at the bottom of the Del Ratón Formation contain clasts of undeformed granitic rocks of 348 ± 2 Ma (Gallastegui et al., 2014) which indicate an early Carboniferous maximum age (Tournaisian) for these deposits. Above the conglomerates, this formation has ages from the Visean (Azcuy et al., 1981; Amenábar and di Pasquo, 2008). The absence of early Carboniferous granites in the Precordillera Cuyana allowed Gallastegui et al. (2014) to propose a source area for these igneous clasts in the hinterland of the Chanic orogen, which would be located further west and southwest, probably in the Frontal Cordillera. The Del Ratón Formation, like all Chanic successions (pre-orogenic and syn-orogenic) located in the Precordillera Cuyana, are deformed by generalized E-vergent structures (Heredia et al., 2018a). This could be explained by the fact that most parts of the Chanic successions of the Precordillera Cuyana were deposited on the eastern wedge (east-vergent wedge) of the Chanic orogenic belt (Fig. 16), developed on the Gondwana margin (former western passive margin of Cuyania). In this margin, ophiolite rocks also crop out, which belong to the small ocean that partially separate

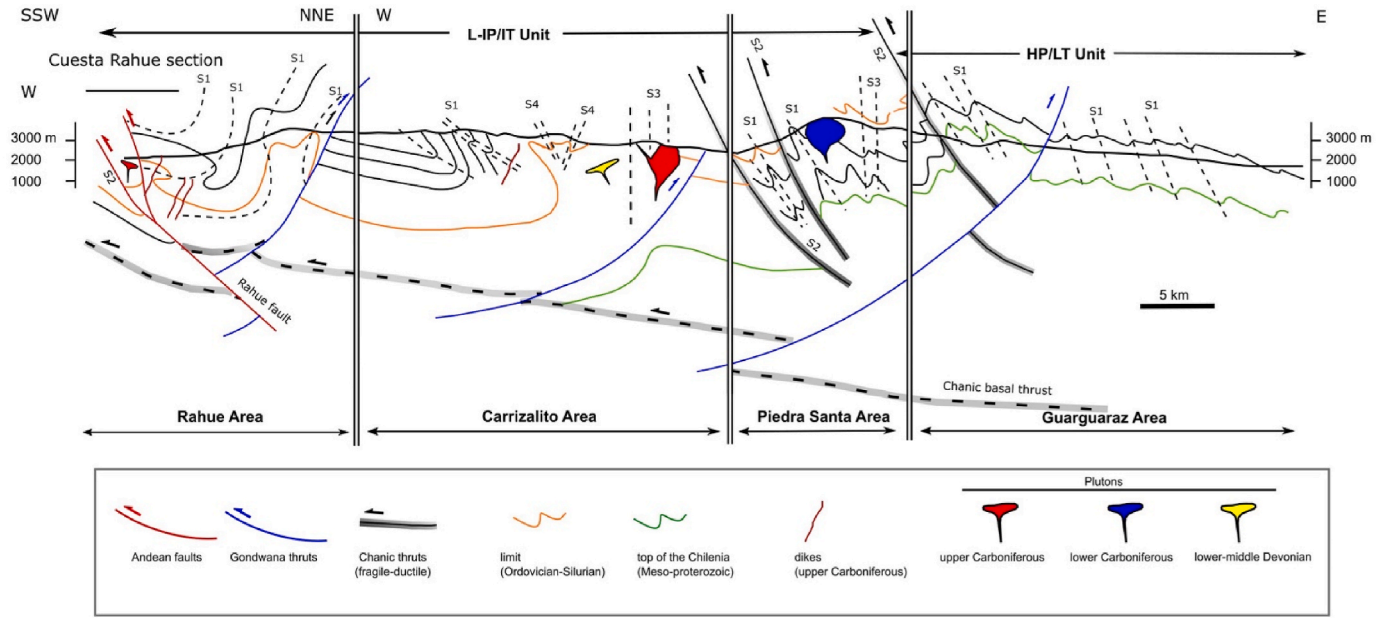

Fig. 14. Schematic cross section of the western wedge (west-vergent wedge) of the Chanic orogen. The vertical lines indicate the different areas that have been used to construct the cross-section; areas whose outcrops are not in continuity. Green line: approximate Cambrian-Ordovician boundary. Orange line: approximate Silurian-Devonian boundary. HP/LT: high pressure and low temperature metamorphism. L-IP/IT: low to intermediate pressure and intermediate temperature metamorphism. Plutonic rocks: in yellow, Early Devonian I-Type granitoids (Chanic pre-orogenic); in blue, early Carboniferous S-Type granitoids (Chanic syn-orogenic); in red, late Carboniferous-early Permian I-Type granitoids (Gondwanan syn-to post-orogenic). The different areas are located in Fig. 1B and C and 16.

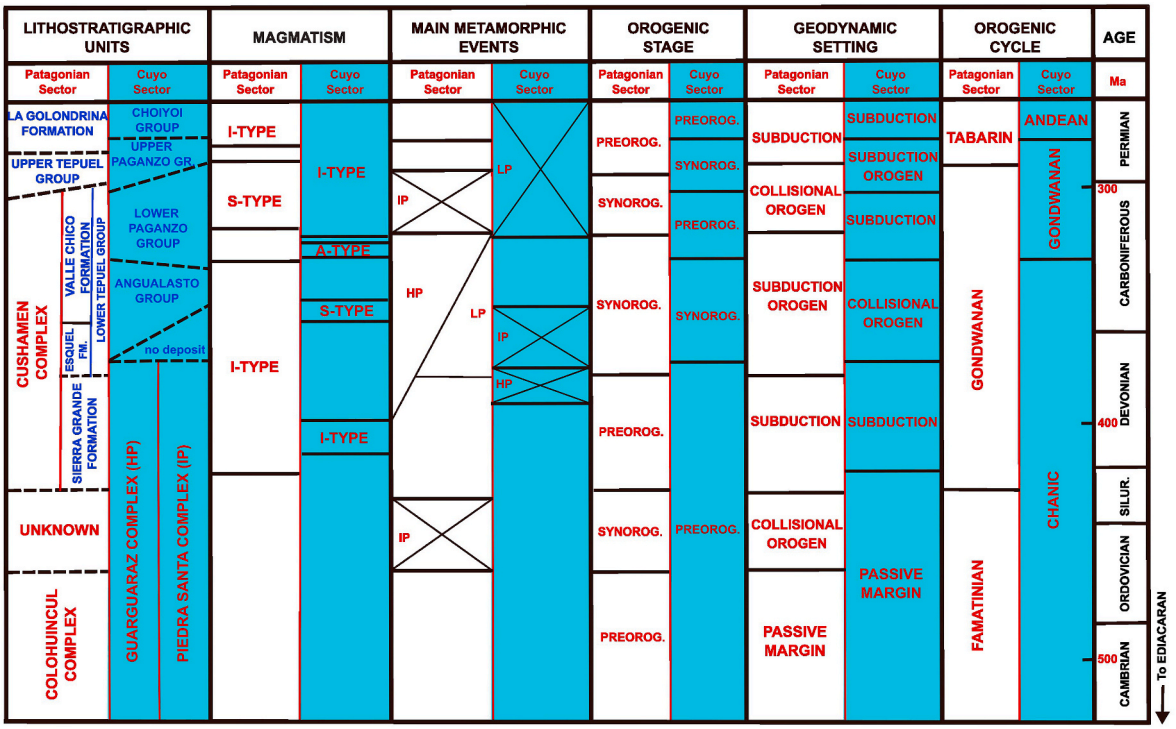

Fig. 15. Correlation sketch of the Paleozoic basements located on both sides of the Huincul lineament: Cuyo Sector (north of 39°S) and Patagonian Sector (south of 39°S). The red and blue letters in the lithostratigraphic units indicate, respectively, metamorphic and sedimentary rocks. HP: High pressure metamorphic conditions. LP: Low Pressure metamorphic conditions. IP: Intermediate pressure metamorphic conditions. In the lithostratigraphic column, the dotted lines indicate major unconformities. Based on data from: Franzese (1995), Limarino et al. (2006), Heredia et al. (2016, 2018a,b) and Serra-Varela et al. (2019, 2021, 2022).

Cuyania from Chilenia (Heredia et al., 2018a). On the contrary, the successions of the Andean Frontal Cordillera, Cordillera del Viento and the Precordillera Neuquina (this work) were developed on the western wedge (west-vergent wedge) of the Chanic orogen, the orogen developed on the eastern active margin of Chilenia, whose general vergence is toward the west (Heredia et al., 2016, 2018a, 2018b). However, in the Cuesta del Rahue area, these vergencies are rather to the NE or NNE, something that will be explained in the Discussion section.

All the series in the study area exhibit a Chanic regional metamorphism (Fig. 16), indicating that they are pre-orogenic. Moreover, the

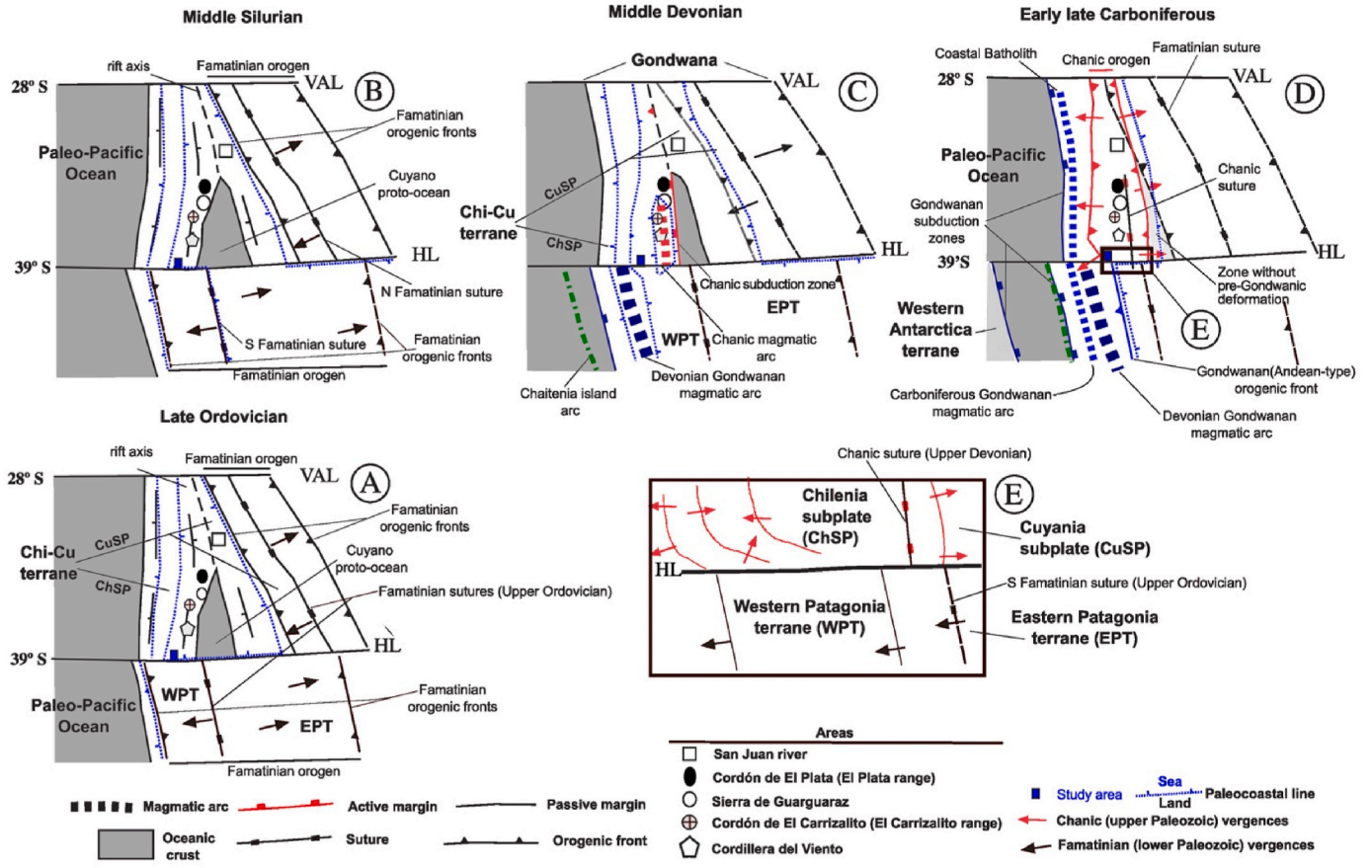

Fig. 16. Geological sketch showing the geodynamic evolution on both sides of the Huincul lineament (Cuyo Sector, north of 39°S and Patagonian sector, south of 39°S), between the Late Ordovician and early Carboniferous (not to scale). WPT: Western Patagonia Terrane; EPT: Esatern Patagonia Terrane; ChSP: Chilenia Subplate of the Chi-Cu Terrane; CuSP: Cuyania Subplate of the Chi-Cu Terrane; VAL: Valle Ancho lineament; HL: Huincul lineament. North of 28°S is where the Puna Sector of the southern Andes Paleozoic basement is located. Modified from Giacosa et al. (2014) and Heredia et al. (2018a).

presence of this metamorphism also indicates that the study area is located in the hinterland of the Chanic orogen, though the low metamorphic grade of the Cuesta del Rahue rocks is indicative of a position further to the foreland than the rocks from Piedra Santa and quite close to the position that would occupy the Cordón del Carrizalito (Fig. 16). In this tectonic context, the foreland of this Chanic orogenic wedge would be located further W to SW of the study area. The rocks from the Piedra Santa range would be located nearer the hinterland, as explained by the presence of medium-grade metamorphism and some early Carboniferous granitoids. These granitoids come from crustal fusion (S-type) according to Rapela et al. (2022) and would have been emplaced in the thickest zones of the Chanic orogen. However, the absence of high-pressure rocks of the former Chanic subduction zone, contrary to the case in Guarguaraz, indicates that the Piedra Santa Area is not located in the innermost part of the Chanic hinterland, close to the Chanic suture. The relative proximity of the Cuesta del Rahue rocks to the rocks from Piedra Santa, and the evident metamorphic gap between both areas, could be tentatively explained by the effect of a ductile thrust that brought the two areas during the Chanic orogeny (Fig. 14).

The presence of undeformed S-type granitoids of early Carboniferous age (ca. 357 Ma) in the syn-orogenic series of the Precordillera Cuyana, indicates that these granites are post-tectonic in relation to the deformation of the internal zones of the Chanic orogen, as can be observed in the study area, but their emplacement must be prior to the deformation of the foreland of this orogen. The deformation of the Chanic foreland must have occurred at the end of the early Carboniferous, not earlier (Fig. 16), so these plutonic rocks should be considered as syn-orogenic igneous rocks. These granitoids were subsequently eroded and transported from the internal zones to the peripheral foreland basins developed on the eastern wedge of the Chanic orogen, where the Angualasto Group (in the sense of Limarino et al., 2006) was deposited (Fig. 15).

Considering all these observations, the Paleozoic rocks of the Cuesta del Rahue area as well as the ones from Piedra Santa range, must correlate with the pre-orogenic series of the Chanic orogenic cycle that crop out north of the Huincul lineament. Specifically, they must correspond to the rocks deposited on the passive eastern margin of Chilenia, which changed to active in the Devonian (Heredia et al., 2018a). Thus, the names used for the lithostratigraphic units defined south of the Huincul lineament must not be used north of this lineament, like the metamorphic complexes of Colohuincul and Cushamen, or the Sierra Grande and Esquel formations (see Serra-Varela et al., 2022) (Fig. 15). Furthermore, since the Chanic pre-orogenic sequences that were deposited on the Chilenia eastern margin are metamorphosed, form isolated outcrops and present varied ages, it is difficult to establish formal lithostratigraphic units and to assign formal names to them. Thus, we propose the term Piedra Santa Complex in order to group these rocks when they have undergone low to intermediate pressure, and the name Guarguaraz Complex to refer to those rocks that underwent high-pressure metamorphism.

In conclusion, the Cuesta del Rahue area would occupy then a position within the western wedge of the Chanic orogen, although in a zone with some retrovergent structures (Figs. 8 and 14). The Cuesta del Rahue area would be located more toward the foreland than the Carrizalito range (Fig. 14), while the Piedra Santa area (with three well-developed cleavages, ductile thrusts and a medium-grade metamorphism) would

be located in an intermediate position between the Sierra de Guarguaraz and the Cordón del Carrizalito, in a very similar position to the Cordillera del Viento area (Fig. 14). Moreover, the Paleozoic rocks of the Cuesta del Rahue and Cordón de Piedra Santa areas show the southernmost evidence of the Chanic collisional deformation (Late Devonian–early Carboniferous), developed under LP-IP/IT metamorphic conditions (Franzese, 1995), which do not seem to be present southwards of the Huincul lineament (Fig. 16), where the pre-Gondwanan deformations are older (early Paleozoic, according to Serra-Varela et al., 2022).

The intense deformation and metamorphism of the Chanic rocks in the Piedra Santa area seem to hamper the development of the structures related to the subsequent Gondwanan subduction-related orogeny (late Carboniferous–early Permian). However, the Gondwanan structures are well developed in the Cuesta del Rahue area, where they affect a large Chanic normal limb and the metamorphism is very low. The Gondwanan orogeny, north of the Huincul lineament and far from the subduction zone, was mainly developed with no metamorphism or with a low-grade metamorphism, under low pressure conditions and close to the Gondwanan magmatic arcs (Heredia et al., 2016). The main structures related to this orogenic event are thrusts and related folds with NNE vergence with some retrovergent structures.

The subduction-related Chachil Plutonic Complex, late Carboniferous–early Permian in age, ca. 303–285 Ma (Varela et al., 1994; Romero et al., 2020), can be correlated with the Gondwanan pulse, also related to subduction, of the Elqui-Limarí Batholith of the Cordillera Frontal (ca. 301–284 Ma, according to Hervé et al., 2014; Sato et al., 2015). This batholith is located between 29° and 31°S and includes syn- and post-orogenic Gondwanan granitoids (Heredia et al., 2016). Moreover, the apophysis of the Chachil Plutonic Complex that crops out in the Cuesta del Rahue area is clearly crosscutting the Chanic and Gondwanan structures. If we also take into account that the Gondwanan deformation ends before ca. 287 Ma in the nearby Cordillera del Viento area (Giacosa et al., 2014), the Chachil Plutonic Complex would be the southernmost extension of the Elqui-Limarí Batholith and the Gondwanan subduction (late early Carboniferous–early Permian) in the southern Cuyo Sector (Heredia et al., 2016).

5. Geodynamic evolution: discussion

The new data and correlations provided in this work, allow us to propose a new model of geodynamic evolution for the Patagonian and Cuyo sectors of the Andean Paleozoic basement surroundings of the Huincul lineament, based in the general model proposed by Heredia et al. (2016) for the Argentinian–Chilean Andes.

From the Ediacaran, the sedimentary rocks of the Southern Neuquén Precordillera, Cordillera del Viento and Frontal Cordillera (between 28° and 39°S, Cuyo Sector) were deposited in the eastern passive margin of the Chilenia subplate (ChSP in Fig. 16A–C) that was separating from the Cuyania subplate (CuSp in Fig. 16A–C), giving rise to a first oceanic crust around 576 Ma. This oceanic crust continued to expand until the end of the Silurian (Davis et al., 1999), forming the Cuyano proto-ocean (Fig. 16A–C). This oceanic crust ends toward the north of the Cuyo Sector, so that both subplates were part of a unique allochthonous terrane, called Chi-Cu by Heredia et al. (2018a) (Fig. 16C), extending up to the Valle Ancho lineament (VAL in Fig. 1B and C and 16) (Heredia et al., 2016), located at 28°S. In the Late Ordovician, the Cuyania subplate collided with the Gondwana margin giving rise to the Famatinian orogen, whose western orogenic front is far from the eastern zone of the study area (Fig. 16). Between the Ediacaran and the Silurian, the extensional passive margins that limited the small Cuyano proto-ocean were filled with thick siliciclastic marine successions, among which some carbonates were interspersed, mostly in the lower part. Several volcanic levels of basic to intermediate nature appear intercalated in this sedimentary series, like the succession that crop out in the Piedra Santa Range (Franzese, 1995). These volcanic additions are more common near the hyper-extended continental margins that surrounded that proto-ocean (López and Gregori, 2004; González-Menéndez et al., 2013), where ultrabasic rocks also appear.

The ending of the Famatinian orogeny around the Silurian–Devonian boundary (ca. 418 Ma) coincides with the beginning of the Chanic subduction, produced below Chilenia, giving rise to a small magmatic arc between ca. 413 and 389 Ma (Dahlquist et al., 2018) (Fig. 16C). Besides, this subduction produced an accretionary prism in whose basal part high pressure and low temperature metamorphic conditions were reached. In the Late Devonian, the oceanic crust that separated Chilenia from Cuyania (the latter being already part of Gondwana) was consumed in the Chanic subduction and both subplates collided, producing the Chanic orogeny that remained active until early Carboniferous times (Fig. 16D). During the last stages of the Chanic subduction or first stages of the subsequent collision, the Chanic basal accretionary prism was exhumed (Willner et al., 2011) and emplaced on the Chilenia margin, giving rise to the Guarguaraz Complex (HP/LT Unit in Fig. 14). Ophiolite units belonging to the former crust of the Cuyano proto-ocean were emplaced on the Cuyania western margin during the Chanic collisional orogeny (ophiolites of the Precordillera Cuyana). The Chanic orogen (Fig. 16D), with a N–S general trend, is relatively narrow and developed the typical double vergence of the collisional orogens. The study area would be located in the west-vergent wedge of this orogen, developed on the eastern margin of Chilenia (Figs. 14 and 16), while the east-vergent eastern wedge is developed in the western margin of Cuyania (Heredia et al., 2016). However, the NE–NNE vergence of the Chanic fold of the Cuesta del Rahue would indicate that it is a retrovergent structure (Fig. 16E). The Chanic orogeny developed internal zones only in its southern part and near the suture zone, where high-grade metamorphic rocks and some early Carboniferous syn-orogenic granites appear (Heredia et al., 2012) (Fig. 16D)., In this context, the Piedra Santa area would be located in the hinterland of the western Chanic wedge. The Cuesta del Rahue outcrops also belong to this hinterland of the Chanic orogen, but due to its very low-grade metamorphism, would be located closer to the foreland. The syn-orogenic basins related to this orogen are only well preserved in the eastern wedge (Precordillera Cuyana), where the Paleozoic rocks of the Chanic orogenic cycle are less covered by the volcanic and sedimentary rocks of the Andean cycle, mostly Mesozoic and Cenozoic.

The WNW–ESE trend of the Chanic orogen structures of the Cuesta del Rahue area, which usually present a N–S disposition farther north (counter-clockwise rotation that exceed 45°), might indicate certain transpression due to their interaction with the Huincul lineament (Fig. 16E). This implies that the Huincul lineament would be active at this time as a left-lateral fault zone, located in the southern end of the western wedge of this orogen. On the contrary, this fault seems to be right lateral in the eastern wedge of the Chanic orogen, evidenced by the change of trend in the Chanic structures, from NNW–SSE in the north (Precordillera Cuyana) to almost N–S in the San Rafael Block, closer to the Huincul lineament (Fig. 16E). The complexity of this structure increases if we consider that part of the rotation of the Chanic structures may have occurred during the Gondwanan and/or Andean deformations, due to a partial reactivation of this fault as oblique or lateral structures respectively (Fig. 16D and E). In relation to this, in Section 3.4.2, a 10°–15° counter-clockwise rotation of the Gondwanan and extensional Andean structures during the Andean orogeny has been described. This rotation implies an original eastern vergence for the large Chanic fold of the Cuesta del Rahue, ratifying its interpretation as a retrovergent structure. On the other hand, Heredia et al. (2016, 2018b) proposed that this lineament is also an important limit to the early Paleozoic Famatinian orogen, since it separates segments of this orogen with different ages and characteristics, as shown in Fig. 16. In this context the current Huincul lineament must be viewed as a large Paleozoic structure with a long history, partially reactivated during the Andean orogeny, as was also described by Ramos et al. (1986), Chernicoff and Zappettini (2004), Mosquera and Ramos (2006) and Ramos

(2008), among others. It is even possible that farther to the east, in zones far away from the study area, the Huincul lineament could have been an older structure that limits the Pampean orogen to the north and the Ross orogen to the south (both Ediacaran–early Cambrian in age), but resolving this topic is beyond the scope of this work.

From the early Carboniferous, a subduction in the new Gondwana margin (former western passive margin of Chilenia) appeared, becoming the precursor of the current Andean subduction (Rebolledo and Charrier, 1994). Starting from the end of the early Carboniferous and mostly during the late Carboniferous and Permian, the Gondwana subduction gave rise to a magmatic arc that migrated from west (Coastal Batholith) to the east (Elqui-Limarí Batolith) (Fig. 16D) (García Sansegundo et al., 2014; Heredia et al., 2018a) and to which the Chachil Plutonic Complex would be related. On this Gondwana margin, thick Carbonifeous siliciclastic sequences were deposited with different depocenters that constitute the lower section of the Paganzo Group (Agua Negra, El Plata, Arroyo del Torreón, Huaraco formations, etc.) (Fig. 15). During the early Carboniferous and the lower part of the late Carboniferous, these sequences were related to an extensional context and developed in zones far away from the incipient Gondwanan subduction (retrowedge basins), in which volcanic intercalations are abundant (A-type magmatism in Fig. 15) (Heredia et al., 2012; Giacosa et al., 2014). This subduction ended with an orogenic process, the Gondwana orogeny of the Cuyo sector, in late Carboniferous–early Permian times, reaching the middle Permian in the northern part of the Cuyo Sector (García-Sansegundo et al., 2014). The Gondwanan syn-orogenic sediments are only preserved in the northern part of the Cuyo Sector (upper Paganzo Group of Fig. 15).

South of the Huincul lineament (Patagonian Sector) and during the Cambrian to middle Silurian, the Andean Paleozoic basement was structured by the Patagonian Famatinian orogenic cycle (Fig. 16A). The Famatinian orogeny of the Patagonia started in Late Ordovician times, very similar to the age of the Cuyo Sector, but it ended at an older age, before the end of the middle Silurian (Wenlock) (Serra-Varela et al., 2019, 2022). This orogeny gave rise to structures with a N–S to NNW–SSE trend and well-developed internal zones. It originated by the accretion of a nearby continental fragment to Gondwana, which was named by Heredia et al. (2016) Western Patagonia terrane (WPT in Fig. 16A). This collision produced the isolation of the Cuyano proto-ocean (Fig. 16A) of the Paleo-Pacific ocean north of the Huincul lineament. When the Patagonian Famatinian orogeny ended, the orogenic belt must have collapsed relatively fast, mainly its eastern wedge, considering that the marine sedimentary rocks of the Silurian–Devonian Sierra Grande Formation (maximum sedimentation age of ca. 428 Ma; Uriz et al., 2011) were deposited over the rocks deformed and metamorphosed during this orogeny (Fig. 16B). At this moment, the Cuyano proto-ocean re-connected with the Paleo-Pacific ocean, located to the south, although this connection zone was developed on the continental crust (Fig. 16B). From the Silurian–Devonian boundary to the early Carboniferous, a large magmatic arc was developed (Serra-Varela et al., 2021 and citation therein) in relation to a new subduction in the Gondwana margin (former western margin of the Western Patagonia terrane) (Fig. 16C). This subduction gave rise to an orogenic process (subduction-related Gondwanan orogeny of Patagonia) between the Late Devonian and the early–late Carboniferous boundary (Pennsylvanian–Mississippian boundary), which could have been initiated by the accretion of an oceanic relief (Chaitenia island arc according to Hervé et al., 2018) to the Gondwana margin (Fig. 16C and D). The subduction-related Gondwanan orogen was developed with scarce metamorphism (only in the areas close to the magmatic arc and the subduction zone) and with a generalized eastward vergence (Fig. 16D), with no consequences on the study area. Syn-orogenic deposits associated with the subduction-related Gondwanan orogeny only crop out south of the Huincul lineament (Heredia et al., 2016). These syn-orogenic sediments are represented by the lower part of the Tepuel Group, formed by the Esquel and Valle Chico formations and their equivalents (Cucchi, 1980; Serra-Varela et al., 2022; Uriz et al., 2022) (Fig. 15).

Later on, between the late Carboniferous and early Permian, the Western Antarctica collision took place (Heredia et al., 2016), (Fig. 16D), which gave rise to the collisional Gondwanan orogen of Patagonia. This orogeny affected the study area beacause it exceeded the boundaries of the Patagonian Sector and the Huincul lineament (Heredia et al., 2016). Farther southwest, this orogeny has a very well-developed hinterland, where syn-orogenic granitoids (S-type) and remains of the Gondwana basal accretionary prism are preserved, although these displaced hundreds of kilometers on the Gondwana margin (García-Sansegundo et al., 2014). Syn-orogenic deposits associated with the collisional Gondwanan orogeny seem to crop out both south and north the Huincul lineament (Heredia et al., 2016). These deposits form the upper part of the Tepuel Group of the Patagonian Sector, constituted by the Pampa de Tepuel and Mojón del Hierro formations and also of the upper section of the Paganzo Group (Limarino et al., 2006), coomposed of the San Ignacio, El Planchón and Patquía formations and their equivalents in the Cuyo Sector (Fig. 15).

Finally, note that there is no evidence that the Huincul lineament could have been an old suture (as proposed by Ramos et al., 1986; Chernicoff and Zappettini, 2004; Ramos, 2008, among others), because the structures and cleavages associated with the different Paleozoic orogenies form a very high angle at both sides (Fig. 16D). In addition, there is no geological or geophysical evidence of ophiolitic rock remains in its surroundings, as already indicated by Gregori et al. (2008). Nevertheless, ophiolitic rocks with a N–S to NNW–SSE disposition appear north of the Huincul lineament, among the Frontal Cordillera, the San Rafel Block, and the Precordillera Cuyana, marking the old Chanic suture (Davis et al., 1999), (Fig. 16D). In this context, and according to Heredia et al. (2016, 2018a,b), the Huincul lineament would rather represent the southern boundary of the Chi-Cu terrane, formed by the Chilenia and Cuyania subplates and the northern boundary of the Western Patagonia and Western Antartica terranes (Fig. 16). This major Paleozoic boundary is only reactivated in some segments and times during the Andean orogenic cycle, such as the Piedra Santa fault near the study area, while other segments appear covered by Mesozoic and/or Cenozoic rocks.

6. Conclusions

The main conclusions of this work are:

- The Paleozoic rocksof the Cuesta del Rahue area constitute a poly-orogenic basement affected by the Chanic (Late-Devonian–early Carboniferous) and Gondwanan (late Carboniferous–early Permian) orogenies during the Paleozoic and the Andean orogeny during the Cenozoic.
- The basement of the Cuesta del Rahue area has a Middle Devonian maximum depositional age (ca. 389 Ma in youngest zircon).
- The sedimentary alternation of sandstones and shales with subordinate conglomerates in this Paleozoic basement is interpreted to be produced in proximal deep-water turbiditic fans. These sediments were probably deposited on the eastern margin of the Chilenia subplate during the Chanic orogenic cycle.
- The presence of a low-grade Chanic metamorphism with only a slaty/rough cleavage development indicates the pre-orogenic character of the Chanic sedimentary sequence and its location in the external hinterland of the N–S Chanic orogenic belt.
- The Chanic structure of the Cuesta del Rahue area is a large normal limb of an asymmetric fold with NNE to NE vergence. Some minor folds developed on this normal limb, such as the tight fold of the Cuesta del Rahue section. This vergence is different to that of the Chanic structures in nearby areas, which are located in the western wedge (west-vergent wedge) of the Chanic orogen (vergence to the W). In our interpretation, the Cuesta del Rahue fold must be a

retrovergent Chanic structure, rotated counterclockwise by the Huincul right-lateral fault, which represents the southern limit of this orogen in the study area. However, the trend of this Chanic structure was possibly also rotated during the Gondwanan and/or Andean orogenies.

- Late Carboniferous (ca. 306 Ma) dikes crosscut the Chanic structures in the Cuesta del Rahue area. In the northwestern part of the neighboring Piedra Santa area, early carboniferous igneous rocks (ca. 357 Ma) also crosscut the Chanic structures and associated cleavages, affecting rocks that are similar to the ones in Cuesta del Rahue.
- The main Gondwanan structures are folds with NNW–SSE trends that fold the subhorizontal normal limb of the large asymmetric Chanic fold and its related cleavage. NNE- and SSW-directed reverse faults and their associated folds affecting late Carboniferous dykes also appear in the study area.
- The Andean structures are related to a pre-orogenic Mesozoic extensional regime and to the development of the Aluminé thrust and fold belt. In the Cuesta del Rahue area the Andean extensional structures are small-scale extensional folds and NNE- and SSW-dipping normal faults. The main Andean contractional structure is the NW–SE Rahue fault, which links the E–W Piedra Santa tear fault with the NNE–SSW Catán Lil reverse fault. The Rahue fault have a ~SW tectonic transport direction, uplifting the Cuesta del Raue area and superimposing Paleozoic rocks on top of Mesozoic and Cenozoic rocks.
- The Piedra Santa fault partially reactivated the Huincul right-lateral and left-lateral Chanic faults that establish the southern limit of both wedges of the Chanic orogen, giving rise to the current Huincul lineament.
- In the study area, the Huincul lineament represents a Paleozoic Chanic structure only reactivated in some segments by the Gondwanan and/or Andean orogenies. South of this lineament, the Chanic deformation disappears, and the pre-Gondwanan compressive deformation is the older Famatinian Patagonian orogeny, Late Ordovician–middle Silurian in age.
- The Cuesta del Rahue area represents the southernmost outcrop of the N–S Chanic orogenic belt and also of the Chilenia subplate, whose collision with Gondwana developed this orogen. In this context, the E–W Huincul lineament is not a suture, since the suture has N–S trend and is located further east, between the Hihg Cordillera of the Andes and the Precordillera/San Rafael Block.
- We propose the name Piedra Santa Complex for the pre-orogenic rocks developed under LP-IP metamorphic conditions during the Chanic cycle in the western wedge of the Chanic orogenic belt. For the Chanic metamorphic rocks developed under HP metamorphic conditions and located more toward the hinterland, we propose the name Guarguaraz Complex.
- Based on all the new data collected and previous works, we propose a new geodynamic evolution model for the area located at the boundary between the Cuyo and Patagonian sectors of the Andean Paleozoic basement.

CRediT authorship contribution statement

Nemesio Heredia: Writing – review & editing, Supervision, Investigation, Funding acquisition. **David Pedreira:** Writing – review & editing, Writing – original draft, Investigation, Data curation. **Raúl Giacosa:** Writing – original draft, Validation, Investigation, Data curation. **Samanta Serra-Varela:** Writing – original draft, Investigation, Data curation. **Nicolás Foix:** Writing – original draft, Investigation, Data curation. **José Allard:** Writing – original draft, Investigation. **Pablo González:** Writing – original draft, Investigation. **Fidel Martín-González:** Writing – original draft, Investigation.

Declaration of competing interest

The authors declare that they have no known competing financial interests or personal relationships that could have appeared to influence the work reported in this paper.

Data availability

Data will be made available on request.

Acknowledgments

This work has been supported by the projects TORANDES (CGL2012-38396-C03) of the Spanish I + D + i Plan with FEDER Funds of the European Union and PIP-CONICET 112-201101-00324 of Argentina. This is a contribution of the GEOTEC Group, with additional funding from the European Regional Development Funds and the Government of the Principality of Asturias (IDI/2018/000216 and AYUD/2021/51923). The authors thank the technical and human support provided by SGIker of UPV/EHU and European funding (ERDF and ESF). We are specially grateful to Romina Sulla for reviewing the English text of the manuscript. We also thank A. Folguera and M. Naipauer for their comments and suggestions that have improved the original manuscript.

References

Amenábar, C., di Pasquo, M., 2008. Nuevos aportes a la palinología, cronología y paleoambientes de la Precordillera Occidental de Argentina: formaciones El Planchón, Codo (Devónico) y El Ratón (Mississippiano). Acta Geol. Lilloana 21 (1), 3–20.

Azcuy, C.L., Cesari, S.N., Longobucco, M.I., 1981. Las plantas fósiles de la Formación el Ratón (provincia de San juan). Ameghiniana 18, 11–28.

Bechis, F., Cristallini, E., Giambiagi, L., Yagupsky, D.L., Guzmán, C.G., García, V.H., 2014. Transtensional tectonics induced by oblique reactivation of previous lithospheric anisotropies during the Late Triassic to Early Jurassic rifting in the Neuquén basin: insights from analog models. J. Geodyn. 79, 1–17.

Caminos, R., 1965. Geología de la vertiente oriental del Cordón del Plata, Cordillera Frontal de Mendoza. Rev. Asoc. Geol. Argent. 20 (3), 351–392.

Chernicoff, C.J., Zappettini, E., 2004. Geophysical evidence for terrane boundaries in south-central Argentina. Gondwana Res. 8 (4), 1105–1116.

Cingolani, C.A., Dalla Salda, L., Hervé, F., Munizaga, F., Pankhurst, R., Parada, M., Rapela, C., 1991. The Magmatic Evolution of Northern Patagonia; New Impressions of Pre-andean and Andean Tectonics, vol. 265. Geological Society of America, Special Paper, pp. 29–44.

Cingolani, C.A., Zanettini, J.C., Leanza, H.A., 2011. El basamento ígneo y metamórfico. In: Leanza, H.A., Arregui, C., Carbone, O., Danieli, J.C., Vallés, J. (Eds.), Geología y Recursos Naturales de la Provincia del Neuquén, vol. 4. Asociación Geológica Argentina, Buenos Aires, pp. 37–48.

Colombo, F., Limarino, C.O., Spalletti, L.A., Busquets, P., Cardó, R., Méndez-Bedia, I., Heredia, N., 2014. Late palaeozoic lithostratigraphy of the andean Precordillera revisited (san juan province, Argentina). J. Iber. Geol. 40 (2), 241–259.

Cucchi, R.J., 1980. La Formación Esquel: nueva interpretación estratigráfica. Rev. Asoc. Geol. Argent. 35 (2), 167–173.

Cucchi, R.J., Leanza, H., Repol, D., Escosteguy, L., González, R., Danielli, J.C., 2005. Hoja Geológica 3972-IV (Junín de los Andes) provincia del Neuquén, vol. 357. Servicio Geológico Minero Argentino, Boletín, Buenos Aires, p. 102.

Davis, J.S., Roeske, S., McClelland, W., Snee, L.W., 1999. Closing the ocean between the Precordillera terrane and Chilenia: early Devonian ophiolite emplacement and deformation in the southwest Precordillera. In: Ramos, V., Keppie, J. (Eds.), Laurentia and Gondwana Connections before Pangea, vol. 336. Geological Society of America, Special Paper, pp. 115–138.

Davis, J.S., Roeske, S., McClelland, W., Kay, S.M., 2000. Mafic and ultramafic crustal fragments of the southwestern Precordillera terrane and their bearing on tectonic models of the early Paleozoic in western Argentina. Geology 28, 171–174.

Dahlquist, J.A., Alasino, P.H., Basei, M.A.S., Morales-Cámera, M.M., Macchioli-Grande, M., Campos-Neto, M.C., 2018. Petrological, geochemical, isotopic, and geochronological constraints for the Late Devonian–Early Carboniferous magmatism in SW Gondwana (27–32°LS): an example of geodynamic switching. Int. J. Earth Sci. 107, 2575–2603.

Dickinson, W.R., Gehrels, G.E., 2009. Use of U-Pb ages of detrital zircons to infer maximum depositional ages of strata: a test against a Colorado Plateau Mesozoic database. Earth Planet Sci. Lett. 288 (1–2), 115–125.

Digregorio, J.H., Uliana, M.A., 1980. Cuenca Neuquina. Geología Regional Argentina 2, 985–1032 (Academia Nacional de Ciencias, Córdoba).

Folguera, A., Etcheverria, M., Pazos, P., Giambiagi, L., Cortés, J.M., Fauqué, L., Fusari, C., Rodriguez, M.F., 2003. Hoja de la Carta Geológica de la República Argentina a escala 1:100.000 N° 3369-15, Potrerillos. Servicio Geológico Minero Argentino (SEGEMAR), p. 262.

Franzese, J.R., 1995. El Complejo Piedra Santa (Neuquén, Argentina): parte de un cinturón metamórfico neopaleozoico del Gondwana suroccidental. Rev. Geol. Chile 22 (2), 193–202.
Franzese, J.R., Veiga, G.D., Muravchik, M., Ancheta, D., Elia, L.D., 2007. Estratigrafía de'sin-rift' (Triásico Superior - jurásico Inferior) de la Cuenca Neuquina en la sierra de Chacaico, Neuquén. Argentina. Revista Geológica de Chile 34 (1), 49–62.
Franzese, J.R., D'Elia, L., Bilmes, A., Muravchik, M., Hernández, M., 2011. Superposición de cuencas extensionales y contraccionales oligo-miocenas en el retroarco andino norpatagónico: la Cuenca de Aluminé, Neuquén, Argentina. Andean Geol. 38 (2), 319–334.
Gallastegui, G., González-Menéndez, L., Rubio-Ordóñez, A., Cuesta, A., Gerdes, A., 2014. Origin and provenance of igneous clasts from late Palaeozoic conglomerate formations (Del Ratón and El Planchó. the Andean Precordillera of San Juan, Argentina. Journal of Iberian Geology 40 (2), 261–282.
García Morabito, E., Ramos, V., 2012. Andean evolution of the Aluminé fold and thrust belt, northern patagonian Andes (38°30′-40°30′S). J. S. Am. Earth Sci. 38, 13–30.
García-Sansegundo, J., Farias, P.J., Rubio Ordóñez, A., Heredia, N., 2014. The Palaeozoic basement of the Andean Frontal Cordillera at 34° S (Cordón del Carrizalito, Mendoza Province, Argentina): geotectonic implications. J. Iber. Geol. 40 (2), 321–330.
García-Sansegundo, J., Gallastegui, G., Farias, P., Rubio-Ordóñez, A., Cuesta, A., Heredia, N., Giambiagi, L.B., Clariana, P., 2016. Evolución tectono-metamórfica Chánica del Complejo Guarguaraz, Cordillera Frontal de los Andes (Mendoza, Argentina). Geotemas 16 (2), 427–430.
Garrido, M., Barra, F., Dominguez, E., Ruiz, J., Valencia, V., 2008. Late Carboniferous porphyry copper mineralization at La Voluntad, Neuquén, Argentina: constraints from Re–Os molybdenite dating. Miner. Deposita 43, 591–597.
Giacosa, R., Heredia, N., 2004. Structure of the North Patagonian thick-skinned fold-and-thrust belt, southern central Andes, Argentina (41°-42°S). J. S. Am. Earth Sci. 18, 61–72.
Giacosa, R.E., Afonso, J.C., Heredia, N., Paredes, J., 2005. Tertiary tectonics of the sub-Andean region of the North Patagonian Andes, southern central Andes of Argentina (41°- 42°30'S). J. S. Am. Earth Sci. 20, 157–170.
Giacosa, R.E., Allard, J., Foix, N., Heredia, N., 2014. Stratigraphy, structure and geodynamic evolution of the Paleozoic rocks in the Cordillera del Viento (37°S latitude, Andes of Neuquén, Argentina). J. Iber. Geol. 40 (2), 331–348.
Giambiagi, L.B., Mescua, J.F., Heredia, N., Farias, P., García-Sansegundo, J., Fernández, C., Stier, S., Pérez, D.J., Bechis, F., Moreiras, S.M., Lossada, A., 2014. Reactivation of Paleozoic structures during Cenozoic deformation in the Cordón del Plata and Southern Precordillera ranges (Mendoza, Argentina). J. Iber. Geol. 40, 309–320.
González-Menéndez L, Gallastegui, G., Cuesta, A., Heredia, N., Rubio-Ordóñez A, 2013. Petrogenesis of Early Paleozoic basalts and gabbros in the western Cuyania terrane: constraints on the tectonic setting of the southwestern Gondwana margin (Sierra del Tigre, Andean Argentine Precordillera). Gondwana Res. 24 (1), 359–376.
Gregori, D.A., Kostadinoff, J., Strazzere, L., Raniolo, A., 2008. Tectonic significance and consequences of the Gondwanide orogeny in northern Patagonia, Argentina. Gondwana Res. 14, 429–450.
Guzmán, C., Tapia, F., Ambrosio, A., Gutiérrez-Pleimling, A., Bustos, G., Gómez, C., González, J.M., 2021. Lower jurassic deformation in the eastern Huincul high, Argentina. J. S. Am. Earth Sci. 109, 103295.
Heredia, N., Farias, P., García-Sansegundo, J., Giambiagi, L.B., 2012. The Basement of the Andean Frontal Cordillera in the Cordón del Plata (Mendoza, Argentina): geodynamic evolution. Andean Geol. 39, 242–257.
Heredia, N., García-Sansegundo, J., Gallastegui, G., Farias, P., Giacosa, R., Alonso, J.L., Busquets, P., Charrier, R., Clariana, P., Colombo, F., Cuesta, A., Gallastegui, J., Giambiagi, L., González-Menéndez, L., Limarino, C.O., Martín-González, F., Pedreira, D., Quintana, L., Rodríguez-Fernández, L.R., Rubio-Ordóñez, A., Seggiaro, R., Serra-Varela, S., Spalletti, L., Cardó, R., Ramos, V.A., 2016. Evolución Geodinámica de los Andes de Argentina, Chile y la Península Antártica durante el Neoproterozoico superior y el Paleozoico. Trab. Geol. 35, 237–278.
Heredia, N., García-Sansegundo, J., Gallastegui, G., Farias, P., Giacosa, R., Giambiagi, L., Busquets, P., Colombo, F., Charrier, R., Cuesta, A., Rubio-Ordóñez, A., Ramos, V.A., 2018a. Review of the geodynamic evolution of the SW margin of Gondwana preserved in the Central Andes of Argentina and Chile (28°-38° S latitude). J. S. Am. Earth Sci. 87, 87–94.
Heredia, N., García-Sansegundo, J., Gallastegui, G., Farias, P., Giacosa, R., Hongn, F., Tubía, J.M., Juis Alonso, J., Busquets, P., Charrier, R., Clariana, P., Colombo, F., Cuesta, A., Gallastegui, J., Giambiagi, L., González-Menéndez, L., Limarino, O., Martín-González, F., Pedreira, D., Quintana, L., Rodríguez-Fernández, L.R., Rubio-Ordoñez, A., Seggiario, R., Serra-Varela, S., Spalletti, L., Cardó, R., Ramos, V.A., 2018b. In: Folguera, A., Contreras Reyes, A., Heredia, N., Encinas, A., Oliveros, V., Dávila, F., Collo, G., Giambiagi, L., Maksymowicz, A., Iglesia Llanos, M.P., Turienzo, M., Naipauer, M., Orts, D., Litvak, V., Alvarez, O., Arriagada, C. (Eds.), The Pre-andean Phases of Construction of the Southern Andes Basement in Neoproterozoic-Paleozoic Times. The evolution of the Chilean-Argentinean Andes, Switzerland. Springer-Verlag, pp. 111–131.
Hernández, N., Galetto, A., Cristallini, E., García, V., Bechis, F., Giambiagi, L., 2022. Late Triassic-Early Jurassic extensional tectonics in the Neuquén Basin (Argentina). New insights from stratigraphic and structural analyses of the Chachil depocenter (39°S). J. Struct. Geol. 154, 104483.
Hervé, F., Fanning, C.M., Calderón, M., Mpodozis, C., 2014. Early permian to late triassic batholiths of the Chilean frontal cordillera (28°-31°S): SHRIMP U-Pb zircon ages and Lu-Hf and O isotope systematic. Lithos 184–187, 436–446.
Hervé, F., Calderón, M., Fanning, C.M., Pankhurst, R.J., Rapela, C.W., Quezada, P., 2018. The country rocks of Devonian magmatism in the north Patagonian Massif and Chaitenia. Andean Geol. 45, 301–317.
Jackson, S.E., Pearson, N.J., Griffin, W.L., Belousova, E.A., 2004. The application of laser ablation-inductively coupled plasma-mass spectrometry to in situ U-Pb zircon geochronology. Chem. Geol. 211 (1–2), 47–69.
Leanza, H.A., 1992. Estratigrafía del Paleozoico y Mesozoico anterior a los Movimientos Intermálmicos en la comarca del Cerro Chachil, provincia del Neuquén. Rev. Asoc. Geol. Argent. 45 (3–4), 272–299.
Leanza, H.A., Hugo, C.A., Herrero, J.C., Donnari, E., Pucci, J.C., 1997. Hoja Geológica 3969-III Picún Leufú, provincias de Neuquén y Río Negro, vol. 218. Servicio Geológico Minero Argentino, Boletín, Buenos Aires, p. 128.
Leanza, H.A., Llambías, E.J., Carbone, O., 2005. Unidades estratigráficas limitadas por discordancias en los depocentros de la Cordillera del Viento y la Sierra de Chacaico durante los inicios de la Cuenca Neuquina, CD Edition. 6° Congreso de Exploración y Desarrollo de Hidrocarburos, Mar del Plata, Argentina, p. 23.
Limarino, C., Tripaldi, A., Marenssi, S., Fauqué, L., 2006. Tectonic, sea level, and climatic controls on Late Paleozoic sedimentation in the western basins of Argentina. J. S. Am. Earth Sci. 22, 205–226.
López, V., Gregori, D.A., 2004. Provenance and evolution of the Guarguaraz complex, cordillera frontal, Argentina. Gondwana Res. 7, 1197–1208.
López de Azarevich, V.L., Escayola, M., Azarevich, M.B., Pimentel, M.M., Tassinari, C., 2009. The Guarguaraz Complex and the Neoproterozoic-Cambrian evolution of the southwestern Gondwana: geochemical signature and geochronological constrains. J. S. Am. Earth Sci. 28, 333–344.
Loske, W., Márquez, M., Giacosa, R., Pezzuchi, H., Fernández, M.I., 1999. U/Pb geochronology of pre-Permian Basement Rocks in the Macizo del Deseado, Santa Cruz province, Argentine Patagonia, vol. 1. XV Congreso Geológico Argentino, Actas, Salta, Argentina), pp. 102–103.
Ludwig, K.R., 2003. User's Manual for Isoplot 3.00-A Geochronological Toolkit for Microsoft Excel. Berkeley Geochronology Center Special Publication, p. 74.
Massonne, H.J., Calderón, M., 2008. P-T evolution of metapelites from the Guarguaraz Complex, Argentina: evidence for Devonian crustal thickening close to the western Gondwana margin. Rev. Geol. Chile 35 (2), 215–231.
Meinhold, G., Kostopoulos, D., Frei, D., Himmerkus, F., Reischmann, T., 2010. U–Pb LA-SF-ICP-MS zircon geochronology of the Serbo-Macedonian Massif, Greece: palaeotectonic constraints for Gondwana-derived terranes in the Eastern Mediterranean. Int. J. Earth Sci. 99, 813–832.
Mosquera, A., Ramos, V.A., 2006. Intraplate deformation in the Neuquén embayment. In: Kay, S.M., Ramos, V.A. (Eds.), Evolution of an Andean Margin: A Tectonic and Magmatic View from the Andes to the Neuquén Basin (35°-39°S Lat), vol. 407. Geological Society of America, Special Paper, pp. 97–123.
Mosquera, A., Silvestro, J., Ramos, V., Alarcón, M., Zubiri, M., 2011. In: Leanza, H.A., Arregui, C., Carbone, O., Danieli, J.C., Vallés, J.M. (Eds.), La estructura de la dorsal de Huincul. Geología y Recursos Naturales de la provincia del Neuquén. Asociación Geológica Argentina, pp. 385–397.
Mutti, E., Bernoulli, D., Ricci Lucchi, F., Tinterri, R., 2009. Turbidites and turbidity currents from Alpine 'flysch' to the exploration of continental margins. Sedimentology 56, 267–318.
Naipauer, M., García Morabito, E., Marques, J.C., Tunik, M., Rojas Vera, E.A., Vujovich, G.I., Pimentel, M.P., Ramos, V.A., 2012. Intraplate Late Jurassic deformation and exhumation in western central Argentina: constraints from surface data and U-Pb detrital zircon ages. Tectonophysics 524–525, 59–75.
Naipauer, M., García Morabito, E., Manassero, M., Valencia, V.V., Ramos, V.A., 2018. In: Folguera, A., Contreras Reyes, A., Heredia, N., Encinas, A., Oliveros, V., Dávila, F., Collo, G., Giambiagi, L., Maksymowicz, A., Iglesia Llanos, M.P., Turienzo, M., Naipauer, M., Orts, D., Litvak, V., Alvarez, O., Arriagada, C. (Eds.), A Provenance Analysis from the Lower Jurassic Units of the Neuquén Basin. Volcanic Arc or Intraplate Magmatic Input?. The evolution of the Chilean-Argentinean Andes, Switzerland. Springer-Verlag, pp. 191–222.
Pankhurst, R.J., Rapela, C.W., Fanning, C.M., Márquez, M., 2006. Gondwanide continental collision and the origin of Patagonia. Earth Sci. Rev. 76, 235–257.
Paton, C., Hellstrom, J., Paul, B., Woodhead, J., Hergt, J., 2011. Iolite: freeware for the visualisation and processing of mass spectrometric data. J. Anal. At. Spectrom. 26, 2508–2518.
Petrus, J.A., Kamber, B.S., 2012. VizualAge: a novel approach to laser ablation ICP-MS U-Pb geochronology data reduction. Geostand. Geoanal. Res. 36 (3), 247–270.
Puelles, P., Abalos, B., García de Madinabeitia, S., Sánchez-Lorda, M.E., Fernández-Armas, S., Gil Ibarguchi, J.I., 2014. Provenance of quartz-rich metamorphic tectonite pebbles from the Black Flysch (W Pyrenees, N Spain): an EBSD and detrital zircon LA-ICP-MS study. Tectonophysics 632 (C), 123–137.
Pujols, E.J., Leva-López, J., Stockli, D.F., Rossi, V.M., Steel, R.J., 2018. New insights into the stratigraphic and structural evolution of the middle Jurassic S. Neuquén Basin from Detrital Zircon (U-Th)/(He-Pb) and Apatite (U-Th)/He ages. Basin Res. 30 (6), 1280, 1279.
Ramos, V.A., 2008. Patagonia: a Paleozoic continental adrift? J. S. Am. Earth Sci. 26 (3), 235–251.
Ramos, V.A., Folguera, A., García Morabito, E., 2011. Las provincias geológicas del Neuquén. In: Leanza, H.A., Arregui, C., Carbone, O., Danieli, J.C., Vallés, J.M. (Eds.). Geología y Recursos Naturales de la provincia del Neuquén. Asociación Geológica Argentina, pp. 317–326.
Ramos, V.A., Jordan, T.E., Allmendinger, R.W., Mpodozis, C., Kay, S.M., Cortés, J.M., Palma, M.A., 1986. Paleozoic terranes of the central Argentine-Chilean Andes. Tectonics 5 (6), 855–880.
Ramos, V.A., García Morabito, E., Hervé, F., Fanning, C.M., 2010. Grenville-age sources in Cuesta Rahue, northern Patagonia: constrains from U-Pb/SHRIMP ages from detrital zircons. International Geological Congress on the Southern Hemisphere (GEOSUR 2010), Absqtracts. Bollettino di Geofisica Teorica ed Applicata 51 (Suppl. ment), 42–44.

Rapela, C.W., Hervé, F., Pankhurst, R.J., Calderón, M., Quezada, P., 2022. The Chaitenia Accretionary Orogen of Northwest Patagonia: New U-Pb SHRIMP Ages of the Foreland Domain. XXI Congreso Geológico Argentino, Actas, pp. 1511–1512 (Puerto Madryn, Argentina).

Rebolledo, S., Charrier, R., 1994. Evolución del basamento paleozoico en el área de Punta Claditas, Región de Coquimbo, Chile (31°-32° S). Rev. Geol. Chile 21, 55–69.

Rodríguez-Fernández, L.R., Heredia, N., García Espina, R., Cegarra, M.I., 1997. Estratigrafía y estructura de los Andes Centrales argentinos entre los 30° y 31° de latitud Sur. In: Busquets, P., Colombo, F., Pérez-Estaún, A. (Eds.), Geología de los Andes Centrales, Acta Geológica Hispánica 32 (1–2), 51–75.

Romero, R., Barra, F., Leisena, M., Salazar, E., González-Jiménez, J.M., Reich, M., 2020. Sedimentary provenance of the Late Paleozoic metamorphic basement, south-central Chile: implications for the evolution of the western margin of Gondwana. Int. Geol. Rev. 62 (5), 1–16.

Rossello, E., López de Luchi, M., 2022. Cinemática transpresional pre-andina del segmento Occidental de la Dorsal de Huincul (cerro Lotena – cerro Granito, Neuquén, Argentina). Revista Asociación Geológica Argentina 79 (3), 473–497.

Sato, A.M., Llambías, E.J., Basei, M.A.S., Castro, C.E., 2015. Three stages in the Late Paleozoic to Triassic magmatism of southwestern Gondwana, and the relationships with the volcanogenic events in coeval basins. J. S. Am. Earth Sci. 63, 48–69.

Serra-Varela, S., González, P.D., Giacosa, R.E., Heredia, N., Pedreira, D., Martín-González, F., Sato, A.M., 2019. Evolution of the Palaeozoic basement of the Northpatagonian Andes in the San Martín de los Andes area (Neuquén, Argentina): petrology, age and correlations. Andean Geol. 46, 102–130.

Serra-Varela, S., Heredia, N., Giacosa, R., García-Sansegundo, J., Farias, P., 2022. Review of the polyorogenic Paleozoic basement of the Argentinean North Patagonian Andes: age, correlations, tectonostratigraphic interpretation and geodynamic evolution. Int. Geol. Rev. 64, 72–95.

Serra-Varela, S., Heredia, N., Otamendi, J., Giacosa, R., 2021. Petrology and geochronology of the San Martín de los Andes batholith: insights into the Devonian magmatism of the North Patagonian Andes. J. S. Am. Earth Sci. 109, 103283.

Sillitoe, R.H., 1977. Permo-Carboniferous, upper Cretaceous and Miocene porphyry copper type mineralization in the Argentinian Andes. Econ. Geol. 72, 99–103.

Sláma, J., Kosler, J., Condon, D.J., Crowley, J.L., Gerdes, A., Hanchar, J.M., Hanchar, J. M., Horstwood, M., Morris, G., Nasdala, L., Norberg, N., Schaltegger, U., Schoene, B., Tubrett, M., Whitehouse, M.J., 2008. Plesovice zircon-A new natural reference material for U-Pb and Hf isotopic microanalysis. Chem. Geol. 249 (1–2), 1–35.

Suárez, M., de la Cruz, R., Fanning, M., Etchart, H., 2008. Carboniferous, Permian and Toarcian magmatism in Cordillera del Viento, Neuquén, Argentina: first U-Pb shrimp dates and tectonic implications. 17° Congreso Geológico Argentino, Actas. San Salvador de Jujuy, Argentina, pp. 906–907.

Ticky, H., Rodríguez Raising, M., Cingolani, C.A., Alfaro, M., Uriz, N., 2009. Graptolitos ordovícicos en el Sur de la Cordillera Frontal de Menzoza. Rev. Asoc. Geol. Argent. 64, 295–302.

Turner, J.C.M., 1976. Descripción Geológica de la Hoja 36a, Aluminé. Carta Geológico-Económica de la República Argentina. Escala 1:200.000. Provincia del Neuquén, vol. 145. Servicio Geológico Nacional, Boletín, Buenos Aires, p. 77.

Uriz, N.J., Cingolani, C.A., Chemale, F., Macambira, M., Armstrong, R., 2011. Isotopic studies on detrital zircons of silurian – devonian siliciclastic sequences from argentinean north Patagonia and sierra de la Ventana regions: comparative provenance. Int. J. Earth Sci. 100, 571–589.

Uriz, N.J., Cingolani, C.A., Taboada, A.C., Arnol, J.A., Basei, M.A., Abre, P., Coelho dos Santos, G.S., 2022. Provenance of pre- and Carboniferous sequences of the Esquel-Arroyo Pescado-Tepuel regions (Argentine Patagonia): a combined U–Pb and Hf isotope study of detrital zircon and constraints on depositional setting. J. S. Am. Earth Sci. 119, 103953.

Varela, R., Texeira, W., Cingolani, C., Dalla Salda, L., 1994. Edad Rubidio - Estroncio de granitoides de Aluminé-Rahue, Cordillera Norpatagónica. Neuquén, Argentina. 7° Congreso Geológico Chileno, Actas vol. 2: pp. 1254-1258. (Concepción, Chile).

Vergani, G.D., Tankard, J., Belotti, J., Welsink, J., 1995. Tectonic Evolution and Paleogeography of the Neuquén Basin, Argentina. In: Tankard, A.J., Suárez, R., Welsink, H.J. (Eds.). Petroleum Basins of South America, American, Association of Petroleum Geologists, pp. 383–402. Memoir 62.

Walker, R.G., 1992. Turbidites and submarine fans. In: Walker, R.G., James, N.P. (Eds.), Facies Models: Response to Sea Level Change. Geological Association of Canada, p. 409.

Willner, A.P., Gerdes, A., Massonne, H.J., Schmidt, A., Sudo, M., Thomson, S.N., Vujovich, G.I., 2011. The geodynamics of collision of a microplate (Chilenia) in Devonian times deduced by the pressure-temperature-time evolution within part of a collisional belt (Guarguaraz Complex, W- Argentina). Contrib. Mineral. Petrol. 162 (2), 303–327.

Zappettini, E., Méndez, V., Zanettini, J.C., 1987. Metasedimentitas mesopaleozoicas en el noroeste de la Provincia del Neuquén. Rev. Asoc. Geol. Argent. 42 (1–2), 206–207.

Zappettini, E., Chernicoff, C., Santos, J., Dalponte, M., Belousova, E., McNaughton, N., 2012. Retrowedge-related Carboniferous units and coeval magmatism in the northwestern Neuquén province, Argentina. Int. J. Earth Sci. 101 (8), 2083–2104.